Table 6
Evaluation of level of concern for human health-risk assessment on the 53 different chemicals.

Level of concern	Number of chemicals with different result based on the different top-concentration limit between r-OECD and ICH TGs (chemical JEC ID)[a]	
Negligible	25	(JEC IDs 3, 4, 6, 19, 28, 33, 36, 39, 44, 45, 47, 57, 66, 69, 74, 75, 76*, 79, 88, 97, 100, 107, 108, 117*, 122)
Minimal	8	(JEC IDs 1*, 16, 55, 62, 64, 78, 85, 119)
Some	16	(JEC IDs 5*, 7*, 10*, 13*, 17*, 35, 51*, 52*, 54*, 73*, 77, 86, 101*, 112*, 118, 121*)
Real	4	(JEC IDs 53*, 71*, 82*, 114*)

Underlined: Ames-positive chemicals.
[a] Positive by the revised OECD test guideline (r-OECD), but negative by the ICH S2(R1) guideline (ICH).
* Evaluated in this paper. Other chemicals without asterisk were evaluated by Morita et al. [9].

Table 7
Distribution of the molecular weights of the 267 or 124 CA-positives from the CGX or JEC database, respectively.

Database	Dataset		Number of chemicals (%) in various ranges of molecular weight					
			<100	100–<200	200–<300	300–<400	400–<500	≥500
CGX	267 CA-positives	210 C	22(10.5)	92(43.8)	60(28.6)	30(14.3)	2(1.0)	4(1.7)
		57 NC	3(5.3)	25(43.9)	15(26.3)	6(10.5)	5(8.8)	3(5.3)
		Total	25(9.4)	117(43.8)	75(28.1)	36(13.5)	7(2.6)	7(2.6)
JEC	124 CA-positives		6(4.8)	79(63.7)	26(21.0)	7(5.6)	2(1.6)	4(3.2)

C, carcinogen; NC, non-carcinogen.

industrial chemicals). These data were supported by a relevance analysis of the *in vitro* CA results (Tables 5 and 6). Fifty-three chemicals, including 15 Ames-positives, were detected as CA-positive with the r-OECD TG, but not with the ICH TG. Twenty-five chemicals were considered to be of negligible concern; thus, a negative call upon the application of the ICH TG was not an issue in such cases. However, the remaining 28 chemicals, of which four chemicals were of real concern (*i.e.*, possible human carcinogens or *in vivo* genotoxins), were not detected as CA-positive under the ICH TG. These results indicate that the ICH TG will miss critical potential carcinogens. Importantly, 15 (*i.e.*, 11 of 15 chemicals of some concern and all four chemicals of real concern) of 28 chemicals of various concern levels were positive in the Ames test, and could be detected with the test-battery system, such as the ICH TG to detect genotoxic carcinogens. No or small changes in the sensitivity/specificity for carcinogenicity or alterations in the number of CA-positives with the r-OECD TG may be explained with the MW analysis of the chemical data set from the CGX and JEC databases. More than half (68.5%) of the CA-positive industrial chemicals had a MW of less than 200, and 90.3% had less than MW 300 in the JEC database (Table 7). Similar results (53.2% < MW 200, 81.3% < MW 300) were shown in the CA-positive data set from the CGX database, which included several pharmaceuticals. Because the MWs of the majority (84.7%) of industrial chemicals are between 100 and 300, 10 mM is considered to be equivalent to 2 mg/mL. Thus, the r-OECD TG showed effects similar to those of the 1997-OECD TG. The top-concentration limit in the ICH TG is 1 mM or 0.5 mg/mL, whichever is lower, although higher test concentrations should be considered for pharmaceuticals with unusually low MWs (*e.g.*, less than 200) [12]. However, no clear recommendation is provided in the ICH TG to determine exactly which 'higher concentrations' should be considered. In the CGX database, 142 chemicals (114 carcinogens and 28 non-carcinogens) had an MW < 200 (Table 7). Of the 142 chemicals, 65 compounds (50 carcinogens and 15 non-carcinogens) were CA-negative upon application of the ICH TG (Table 1). If r-OECD TG were applied to the 65 CA-negatives with MW < 200 (*i.e.*, application of modified ICH TG), 40 of 50 carcinogens and 6 of 15 non-carcinogens would be positive (Table 1). The sensitivity was increased to 58.0% from 45.4%, and the specificity was decreased to 67.8% from 72.9% (Table 3). These values were similar to those after the application of the r-OECD TG. In the JEC database, 85 chemicals were less than MW 200 (Table 7). Forty-seven of the 85 chemicals were negative in the CA test upon application of the ICH TG (Table 2). If r-OECD TG were applied to the 47 CA-negatives with MW < 200, 41 chemicals would be positive (Table 2). The number of CA-positives increased to 101 from 60 upon application of the modified ICH TG (Table 4). The number was similar to that found upon application of the r-OECD TG. This approach suggests the usefulness of applying the r-OECD TG for pharmaceutical substances with MW < 200. Recently, a simulation study performed by Brookmire et al. [10] suggested that lowering the highest concentration on the mg/mL scale to a value close to 2 mg/mL would result in an assay sensitivity close to the 10-mM limit; thus testing up to 5 mg/mL did not increase the sensitivity of the assay. The simulation study suggested also that lowering the current high concentration limit from 10 mM would dramatically impact the sensitivity of the assay. Our analysis with real data was consistent with this simulation study. We also revealed that the top concentration of 2 mg/mL did not decrease the specificity of the assay, although the simulation study did not dictate what the highest concentration should be, or address the specificity. In addition, the lack of significant changes in the sensitivity and specificity after the application of the r-OECD TG suggests that the new top-concentration limit proposed by the r-OECD TG would not affect the evaluation of chromosome damage in in-silico models.

In conclusion, the present analysis suggests that the application of the top-concentration limit (10 mM or 2 mg/mL, whichever is lower) proposed by the r-OECD TG will not affect the sensitivity or specificity of the detection of rodent carcinogens, indicating the validity of the guideline. Thus, the effects on the in-silico evaluation will also be small. However, the r-OECD TG has resulted in little or no reduction in the number of positive chemicals under the 1997-OECD TG, and nearly no improvements in reducing possible false positives for industrial chemicals have been made. Other approaches, *e.g.*, the consideration of the cell systems used, cytotoxicity measurements, non-physiological conditions or metabolic activation systems will be necessary to reduce the number of false positives [5].

Conflict of interests

There are no conflicts of interests.

Acknowledgements

This work was supported by the Health and Labor Sciences Research Grants (H21-Chemical-General-002 and H24-Chemical-Designation-010).

References

[1] Organization for Economic Co-operation and Development (OECD), Guideline for the testing of chemicals, No. 473, In vitro mammalian cell chromosome aberration test, adopted July 21, 1997 (updated). Available at http://www.oecd-ilibrary.org/environment/test-no-473-in-vitro-mammalian-chromosome-aberration-test_9789264071261-en (accessed August 26, 2013).
[2] International Conference on Harmonisation of Technical Requirements for Registration of Pharmaceuticals for Human Use (ICH), S2A guideline, Guidance on genotoxicity testing and data interpretation for pharmaceuticals intended for human use, Step 4 in July 1995.
[3] S.M. Galloway, M.J. Aardema, M. Ishidate Jr., J.L. Ivett, D. Kirkland, T. Morita, P. Mosesso, T. Sofuni, Report from working group on in vitro tests for chromosomal aberrations, Mutat. Res. 312 (1994) 241–261.
[4] D. Scott, S.M. Galloway, R.R. Marshall, M. Ishidate Jr., D. Brusick, J. Ashby, B.C. Myhr, Genotoxicity under extreme culture conditions, a report from ICPEMC task group 9, Mutat. Res. 257 (1991) 147–204.
[5] D. Kirkland, S. Pfuhler, D. Tweats, M. Aardema, R. Corvi, F. Darroudi, A. Elhajouji, H. Glatt, P. Hastwell, M. Hayashi, P. Kasper, S. Kirchner, A. Lynch, D. Marzin, D. Maurici, J. Meunier, L. Müller, G. Nohynek, J. Parry, E. Parry, V. Thybaud, R. Tice, J. van Benthem, P. Vanparys, P. White, How to reduce false positive results when undertaking in vitro genotoxicity testing and thus avoid unnecessary follow-up animal tests: report of an ECVAM workshop, Mutat. Res. 628 (2007) 31–55.
[6] J.M. Parry, E. Parry, P. Phrakonkham, R. Corvi, Analysis of published data for top concentration considerations in mammalian cell genotoxicity testing, Mutagenesis 25 (2010) 531–538.
[7] D. Kirkland, P. Fowler, Further analysis of Ames-negative rodent carcinogens that are only genotoxic in mammalian cells in vitro at concentrations exceeding 1 mM, including retesting of compounds of concern, Mutagenesis 25 (2010) 539–553.
[8] S. Galloway, E. Lorge, M.J. Aardema, D. Eastmond, M. Fellows, R. Heflich, D. Kirkland, D.D. Levy, A.M. Lynch, D. Marzin, T. Morita, M. Schuler, G. Speit, Workshop summary: top concentration for in vitro mammalian cell genotoxicity assays; and report from working group on toxicity measures and top concentration for in vitro cytogenetics assays (chromosome aberrations and micronucleus), Mutat. Res. 723 (2011) 77–83.
[9] T. Morita, M. Honma, K. Morikawa, Effect of reducing the top concentration used in the in vitro chromosomal aberration test in CHL cells on the evaluation of industrial chemical genotoxicity, Mutat. Res. 741 (2012) 32–56.
[10] L. Brookmire, J.J. Chen, D.D. Levy, Evaluation of the highest concentrations used in the in vitro chromosome aberrations assay, Environ. Mol. Mutagen. 54 (2013) 36–43.
[11] ICH, S2(R1) guideline, Guidance on genotoxicity testing and data interpretation for pharmaceuticals intended for human use, Step 4 version, dated 9 November 2011. Available at http://www.ich.org/fileadmin/Public_Web_Site/ICH_Products/Guidelines/Safety/S2_R1/Step4/S2R1_Step4.pdf (accessed August 26, 2013).
[12] OECD, OECD guideline for the testing of chemicals, Proposal for updating test guideline 473, In vitro mammalian chromosome aberration test, December 2013. Available at http://www.oecd.org/env/ehs/testing/TG473_Dec2013_WNT4thCR.pdf.(accessed June 3, 2014).
[13] R. Serafimova, M.F. Gatnik, A. Worth, Review of QSAR models and software tools for predicting genotoxicity and carcinogenicity JRC scientific and technical reports, EUR 24427 EN (2010), Avairable at http://ihcp.jrc.ec.europa.eu/our_labs/predictive_toxicology/doc/EUR_24427_EN.pdf (accessed January 27, 2014).
[14] V.R. Williams, T.R. Naven, A.C. Marchant, A. Hirose, E. Kamata, M. Hayashi, Derek for windows assessment of chromosomal aberration effects, Toxicol. Lett. 164 (Suppl. 1) (2006) 292.
[15] O. Mekenyan, M. Todorov, R. Serafimova, S. Stoeva, A. Aptula, R. Finking, E. Jacob, Identifying the structural requirements for chromosomal aberration by incorporating molecular flexibility and metabolic activation of chemicals, Chem. Res. Toxicol. 20 (2007) 1927–1941.
[16] D. Kirkland, M. Aardema, L. Henderson, L. Müller, Evaluation of the ability of a battery of three in vitro genotoxicity tests to discriminate rodent carcinogens and non-carcinogens I. Sensitivity, specificity and relative predictivity, Mutat. Res. 584 (2005) 1–256.
[17] M. Ishidate Jr., M. Harnois, T. Sofuni, A comparative analysis of data on the clastogenicity of 951 chemical substances tested in mammalian cell cultures, Mutat. Res. 195 (1988) 151–213.
[18] S.M. Galloway, M.J. Armstrong, C. Reuben, S. Colman, B. Brown, C. Cannon, A.D. Bloom, F. Nakamura, M. Ahmed, S. Duk, J. Rimpo, B.H. Margolin, M.A. Resnick, B. Anderson, E. Zeiger, Chromosome aberrations and sister chromatid exchanges in Chinese hamster ovary cells: evaluations of 108 chemicals, Environ. Mol. Mutagen. 10 (Suppl. 10) (1987) 1–175.
[19] K.S. Loveday, M.H. Lugo, M.A. Resnick, B.E. Anderson, E. Zeiger, Chromosome aberration and sister chromatid exchange tests in Chinese hamster ovary cells in vitro: II. Results with 20 chemicals, Environ. Mol. Mutagen. 13 (1989) 60–94.
[20] K.S. Loveday, B.E. Anderson, M.A. Resnick, E. Zeiger, Chromosome aberration and sister chromatid exchange tests in Chinese hamster ovary cells in vitro. V: Results with 46 chemicals, Environ. Mol. Mutagen. 16 (1990) 272–303.
[21] B.E. Anderson, E. Zeiger, M.D. Shelby, M.A. Resnick, D.K. Gulati, J.L. Ivett, K.S. Loveday, Chromosome aberration and sister chromatid exchange test results with 42 chemicals, Environ. Mol. Mutagen. 16 (Suppl. 18) (1990) 55–137.
[22] National Toxicology Program (NTP), NTP website at http://ntp-server.niehs.nih.gov and NTP database search home page at http://tools.niehs.nih.gov/ntp_tox/ (accessed August 26, 2013).
[23] M. Sasaki, K. Sugimura, M.A. Yoshida, S. Abe, Cytogenetic effects of 60 chemicals on cultured human and Chinese hamster cells, Senshokuta (Kromosoma) 20 (1980) 574–584.
[24] M. Ishidate (Ed.), Data Book on Chromosomal Aberration Test, LIC Co., Tokyo, 1987, pp. 19–24 (revised).
[25] M.B. Lioi, M.R. Scarfi, A. Santoro, R. Barbieri, O. Zeni, F. Salvemini, D. Di Berardino, M.V. Ursini, Cytogenetic damage and induction of pro-oxidant state in human lymphocytes exposed in vitro to gliphosphate, vinclozolin, atrazine, and DPX-E9636, Environ. Mol. Mutagen. 32 (1998) 39–46.
[26] A. Matsuoka, A. Matsui, N. Miyata, T. Sofuni, M. Ishidate Jr., Mutagenicity of 3-*tert*-butyl-4-hydroxyanisole (BHA) and its metabolites in short-term tests in vitro, Mutat. Res. 241 (1990) 125–132.
[27] K. Harrington-Brock, C.L. Doerr, M.M. Moore, Mutagenicity of three disinfection by-products: di- and trichloroacetic acid and chloral hydrate in L5178Y/TK+/−−3.7.2C mouse lymphoma cells, Mutat. Res. 413 (1998) 265–276.
[28] A. Matsuoka, K. Yamakage, H. Kusakabe, S. Wakuri, M. Asakura, T. Noguchi, T. Sugiyama, H. Shimada, S. Nakayama, Y. Kasahara, Y. Takahashi, K.F. Miura, M. Hatanaka, M. Ishidate Jr., T. Morita, K. Watanabe, M. Hara, K. Odawara, N. Tanaka, M. Hayashi, T. Sofuni, Re-evaluation of chromosomal aberration induction on nine mouse lymphoma assay "unique positive" NTP carcinogens, Mutat. Res. 369 (1996) 243–252.
[29] H. Reisenbichler, P.M. Eckl, Genotoxic effects of selected peroxisome proliferators, Mutat. Res. 286 (1993) 135–144.
[30] S. Knasmüller, N. Bresgen, F. Kassie, V. Mersch-Sundermann, W. Gelderblom, E. Zöhrer, P.M. Eckl, Genotoxic effects of three Fusarium mycotoxins, fumonisin B1, moniliformin and vomitoxin in bacteria and in primary cultures of rat hepatocytes, Mutat. Res. 13 (1997) 39–48.
[31] H. van den Berghe, Clastogenic effects of haloperidol in vivo and of haloperidol, droperidol and pipamperone in vitro, Arzneim. Forsch. 24 (1974) 2055–2058.
[32] B.L. Kaul, Cytogenetic activity of some common antioxidants and their interaction with X-rays, Mutat. Res. 67 (1979) 239–247.
[33] M.D. Mudry, M. Carballo, M. Labal de Vinuesa, M. Gonzalez Cid, I. Larripa, Mutagenic bioassay of certain pharmacological drugs: III Metronidazole (MTZ), Mutat. Res. 305 (1994) 127–132.
[34] Q.-G. Huang, L.-R. Kong, Y.-B. Liu, L.-S. Wang, Relationships between molecular structure and chromosomal aberrations in in vitro human lymphocytes induced by substituted nitrobenzenes, Bull. Environ. Contam. Toxicol. 57 (1996) 349–353.
[35] A. Matsuoka, T. Sofuni, N. Miyata, M. Ishidate Jr., Clastogenicity of 1-nitropyrene, dinitropyrenes, fluorene and mononitrofluorenes in cultured Chinese hamster cells, Mutat. Res. 259 (1991) 103–110.
[36] U. Egeli, G. Erdogan G., The clastogenic effect of pyrimethamine (Daraprim) on human chromosomes in lymphocyte cultures, Cell Biol. Toxicol. 7 (1991) 347–356.
[37] S.R. Sirianni, Further studies on cytogenetic effects of folpet, Mutat. Res. 53 (1978) 64–265, abstract.
[38] C.A. Hilliard, M.J. Armstrong, C.I. Bradt, R.B. Hill, S.K. Greenwood, S.M. Galloway, Chromosome aberrations in vitro related to cytotoxicity of nonmutagenic chemicals and metabolic poisons, Environ. Mol. Mutagen. 31 (1998) 316–326.
[39] S.M. Galloway, T. Sofuni, M.D. Shelby, A. Thilagar, V. Kumaroo, P. Kaur, D. Gulati, D.L. Putman, H. Murli, R. Marshall, N. Tanaka, B. Anderson, E. Zeiger, M. Ishidate Jr., Multilaboratory comparison of in vitro tests for chromosome aberrations in CHO and CHL cells tested under the same protocols, Environ. Mol. Mutagen. 29 (1997) 189–207.
[40] M.V.U. Rani, M.S. Rao, In vitro effect of fenthion on human lymphocytes, Bull. Environ. Contam. Toxicol. 47 (1991) 316–323.
[41] C. Caballo, A. Herrara, C. Barrueco, A. Santa-Maria, F. Sanz F., E. de la Plena, Analysis of cytogenetic damage induced in CHO cells by the pyrethroid insecticide fenvalerate, Terato. Carcinogen. Mutagen. 12 (1992) 243–249.
[42] M.J. Armstrong, C.L. Bean, S.M. Galloway, A quantitative assessment of the cytotoxicity associated with chromosomal aberration detection in Chinese hamster ovary cells, Mutat. Res. 265 (1992) 45–60.
[43] S.M. Galloway, J.E. Miller, M.J. Armstrong, C.L. Bean, T.R. Skopek, W.W. Nichols, DNA synthesis inhibition as an indirect mechanism of chromosome aberrations: comparison of DNA-reactive and non-DNA-reactive clastogens, Mutat. Res. 400 (1998) 169–186.
[44] B.E. Anderson, E. Zeiger, M.D. Shelby, M.A. Resnick, D.K. Gulati, J.L. Ivett, K.S. Loveday, Chromosome aberration and sister chromatid exchange test results with 42 chemicals, Environ. Mol. Mutagen. 16 (Suppl. 18) (1990) 55–137.
[45] M.D. Shelby, S. Stasiewicz, Chemicals showing no evidence of carcinogenicity in long-term, two-species rodent studies: the need for short-term test data, Environ. Mutagen. 6 (1984) 871–878.

[46] G. Stemp, S. Pascoe, D. Gatehouse, In vitro and in vivo cytogenetic studies of three ß-lactam antibiotics (penicillin VK, ampicillin and carbenicillin), Mutagenesis 4 (1989) 439–445.
[47] Japan Existing Chemical (JEC) database, based on the Chemical Substances Control Low (CSCL), as website at http://dra4.nihs.go.jp/mhlw_data/jsp/SearchPageENG.jsp (accessed August 26, 2013).
[48] Chromosomal aberration test in cultured mammalian cells, 49 Kikyoku no. 392, Law concerning examination and regulation of manufacture, etc. of chemical substances, 1974.
[49] OECD, OECD Existing chemicals database, Website at http://webnet.oecd.org/HPV/UI/Search.aspx (accessed August 26, 2013).
[50] International Agency for Research on Cancer (IARC), IARC monographs on the evaluation of carcinogenic risks to humans, Website at http://monographs.iarc.fr/ (accessed August 26, 2013).
[51] Japan Chemical Industry Ecology Toxicology & Information Center (JETOC), Mutagenicity Test Data of Existing Chemical Substances. Based on the Toxicity Investigation System of the Industrial Safety and Health Law, JETOC, Tokyo, 1996, pp. 86.

DNA Repair 15 (2014) 21–28

Contents lists available at ScienceDirect

DNA Repair

journal homepage: www.elsevier.com/locate/dnarepair

In vivo evidence that phenylalanine 171 acts as a molecular brake for translesion DNA synthesis across benzo[*a*]pyrene DNA adducts by human DNA polymerase κ

Akira Sassa[a,b,1], Tetsuya Suzuki[a,2], Yuki Kanemaru[a,3], Naoko Niimi[a,4], Hirofumi Fujimoto[c], Atsushi Katafuchi[a,5], Petr Grúz[a], Manabu Yasui[a], Ramesh C. Gupta[d], Francis Johnson[d], Toshihiro Ohta[b], Masamitsu Honma[a], Noritaka Adachi[e], Takehiko Nohmi[a,*]

[a] *Division of Genetics and Mutagenesis, National Institute of Health Sciences, 1-18-1 Kamiyoga, Setagaya-ku, Tokyo 158-8501, Japan*
[b] *School of Life Sciences, Tokyo University of Pharmacy and Life Sciences, Hachioji-shi, Tokyo 192-0392, Japan*
[c] *Division of Radiological Protection and Biology, National Institute of Infectious Diseases, 1-23-1 Toyama, Shinjuku-ku, Tokyo 162-8640, Japan*
[d] *Department of Pharmacological Sciences and Department of Chemistry, Stony Brook University, Stony Brook, NY 11794-3400, USA*
[e] *Graduate School of Nanobioscience, Yokohama City University, 22-2 Seto, Kanazawa-ku, Yokohama 236-0027, Japan*

ARTICLE INFO

Article history:
Received 6 October 2013
Received in revised form
10 December 2013
Accepted 29 December 2013
Available online 21 January 2014

Keywords:
Translesion DNA synthesis
DNA polymerase κ
Benzo[*a*]pyrene diolepoxide-N^2-guanine

ABSTRACT

Humans possess multiple specialized DNA polymerases that continue DNA replication beyond a variety of DNA lesions. DNA polymerase kappa (Pol κ) bypasses benzo[*a*]pyrene diolepoxide-N^2-deoxyguanine (BPDE-N^2-dG) DNA adducts in an almost error-free manner. In the previous work, we changed the amino acids close to the adducts in the active site and examined the bypass efficiency. The substitution of alanine for phenylalanine 171 (F171A) enhanced by 18-fold *in vitro*, the efficiencies of dCMP incorporation opposite (−)- and (+)-*trans-anti*-BPDE-N^2-dG. In the present study, we established human cell lines that express wild-type Pol κ (*POLK*+/−), F171A (*POLK* F171A/−) or lack expression of Pol κ (*POLK*−/−) to examine the *in vivo* significance. These cell lines were generated with Nalm-6, a human pre-B acute lymphoblastic leukemia cell line, which has high efficiency for gene targeting. Mutations were analyzed with shuttle vectors having (−)- or (+)-*trans-anti*-BPDE-N^2-dG in the *supF* gene. The frequencies of mutations were in the order of *POLK*−/− > *POLK*+/− > *POLK* F171A/− both in (−)- and (+)-*trans-anti*-BPDE-N^2-dG. These results suggest that F171 may function as a molecular brake for bypass across BPDE-N^2-dG by Pol κ and raise the possibility that the cognate substrates for Pol κ are not BP adducts in DNA but may be lesions in DNA induced by endogenous mutagens.

1. Introduction

The human genome is continuously exposed to a variety of endogenous and exogenous genotoxic agents, which induce DNA damage. These DNA lesions strongly block DNA replication mediated by replicative DNA polymerases (Pols), thereby inducing cell toxicity. Cells have evolved various defense mechanisms against genotoxic agents such as antioxidants, detoxication enzymes, DNA repair and so on. Translesion DNA synthesis (TLS) is one of defense mechanisms to overcome the toxic effects of DNA lesions [1,2]. In fact, human cells possess more than 10 specialized Pols, which can take over the primer DNA from the replicative Pols and continue primer extension beyond the template lesion, i.e., TLS [3–5]. After the successful TLS, the specialized Pols transfer the continued primer DNA to the replicative Pols, what make the chromosome replication complete and rescue the damaged cells [6]. TLS can also suppress mutations by incorporation of correct dNMPs opposite

* Corresponding author. Present address: Biological Safety Research Center, National Institute of Health Sciences, Tokyo 158-8501, Japan. Tel.: +81 3 3700 1564; fax: +81 3 3700 1622.
E-mail address: nohmi@nihs.go.jp (T. Nohmi).
[1] Present address: Laboratory of Structural Biology, NIEHS, 111 T.W. Alexander Drive, Research Triangle Park, NC 27709, USA.
[2] Present address: Division of Health Effects Research, National Institute of Occupational Safety and Health, Kanagawa 214-8585, Japan.
[3] Present address: Division of Toxicology, Department of Pharmacology, Toxicology and Therapeutics, Showa University School of Pharmacy, Tokyo 142-8555, Japan.
[4] Present address: Department of Sensory and Motor Systems, Tokyo Metropolitan Institute of Medical Science, 2-1-6 Kamikitazawa, Setagaya-ku, Tokyo 156-8506, Japan.
[5] Present address: Department of Radiation Life Sciences, Fukushima Medical University, Fukushima 960-1295, Japan.

1568-7864/$ – see front matter © 2014 Elsevier B.V. All rights reserved.
http://dx.doi.org/10.1016/j.dnarep.2013.12.008

the damaged base in the template. A typical example of such error-free TLS is the correct insertion of dAMP opposite thymine dimer induced by ultraviolet light (UV) by human Pol η [7,8]. Defects in the *XPV* gene encoding Pol η are molecular basis for the human genetic disease Xeroderma pigmentosum variant, the sufferers of which are highly susceptible to UV-induced skin cancer. In general, the specialized Pols are less accurate for DNA replication compared to the replicative Pols [9,10]. Therefore, some of TLS mediated by the specialized Pols are error prone and generate sequence changes, i.e., incorrect dNMPs incorporation opposite the damaged template base, thereby causing base substitutions [11,12]. Thus, TLS can be a double-edged sword, as the mechanisms contributing to genetic integrity can themselves result in mutations.

Human Pol κ is one of the specialized Pols and belongs to the Y family, the most predominant Pol family for TLS [6,13–15]. Unlike other Y-family members, i.e., Pol η, Pol ι and REV1, the orthologs of Pol κ present in bacteria, Eukarya and Archaea [16–18]. Other Y-family Pols are present only in Eukarya. Although Pol κ is suggested to be involved in TLS across a number of DNA lesions, i.e., N^2-guanyl adducts induced by polycyclic aromatic hydrocarbons and alkylating agents, a C8-guanyl adduct generated by 2-amino-1-methyl-6-phenylimidazo[4,5-*b*]pyridine (PhIP), the thymine glycol lesion, 8-oxo-guanine and interstrand DNA crosslinks [19–29], the best characterized one is N^2-guanyl adducts induced by benzo[*a*]pyrene (BP). BP is an environmental mutagen that is present in cigarette smoke and released to the air as a combustion product of fossil fuel [30]. Upon contact with lung tissue, BP is metabolized to various reactive intermediates, the most mutagenic and carcinogenic of which is benzo[*a*]pyrene-7,8-dihydrodiol-9,10-epoxide (BPDE) [30,31]. Pol κ appears to be involved in error-free TLS across N^2-guanyl adducts induced by BPDE, i.e., (−)- and (+)-*trans-anti*-BPDE-N^2-dG (hereafter, we call them (−)-BPDE-dG and (+)-BPDE-dG) [19,23,25,32]. Pol κ strongly binds to DNA containing (−)-BPDE-dG, and preferentially incorporates dCMP opposite both (−) and (+) lesions [25]. Several lines of evidence with cultured mammalian cells suggest that Pol κ is involved in error-free TLS across BPDE DNA adducts *in vivo* [24,33,34]. However, the catalytic mechanism underlying the error-free TLS across the lesions is not fully understood yet.

To understand better the catalytic mechanism, we have replaced amino acids proximal to the adducts with alanine and examined the TLS activities of the purified enzymes *in vitro* [35]. The amino acids that were replaced were phenylalanine 171 (F171), arginine 175 (R175) and leucine 197 (L197), based on the ternary complex of Pol κ with DNA and an incoming nucleotide [36]. R175 to alanine (R175A) and L197 to alanine (L197A) exhibited either no or a slight decrease in their effects on the TLS activities. Unexpectedly, however, the substitution of F171 to alanine (F171A) increased the TLS activities by about 20 fold and significantly enhanced the binding ability to DNA containing (−)-BPDE-dG. In the present study, we established human cells that express the F171A variant Pol κ and examined the sensitivity to (−)- and (+)-BPDE-dG in DNA. Such cells exhibited significantly lower mutation frequencies induced by the adducts compared to the cells expressing wild-type Pol κ. From the current *in vivo* studies along with our previous *in vitro* results, we conclude that F171 acts as a molecular brake for Pol κ-mediated TLS across (−)- and (+)-BDPE-dG in DNA. A possible mechanism by which F171 inhibits TLS across BPDE adducts in DNA and possible cognate substrates for Pol κ are discussed.

2. Materials and methods

2.1. Cell culture and DNA transfection

The human pre-B cell line Nalm-6 and its derivatives were cultured in RPMI 1640 (Nacalai Tesque) with 10% calf serum (Thermo Fisher Scientific) and 50 μM 2-mercaptoethanol at 37 °C in an atmosphere of 5% CO_2 and 100% humidity. DNA transfection for gene targeting was performed as previously described [37]. Briefly, the linearized targeting construct DNA (2 μg) was transfected into 2.0×10^6 cells that were suspended in 0.1 mL of KitT solution with supplement 1 by using the Nucleofector I according to the manufacturer's instructions (Lonza). After cultivation for 24–48 h, the cells were re-plated at a density of ~10^6 per 90-mm dish at agarose medium containing 400 μg/ml hygromycin B (Wako) or 0.5 μg/ml puromycin (Wako). Alternatively, the appropriate numbers of cells were plated into 96-well plates in medium containing one or other of the same medium. After 2–3 weeks incubation, the resulting drug resistant colonies were isolated and cultured for stock frozen permanents for preparation of cell extracts, total RNA and genomic DNA.

2.2. Targeting constructs for POLK knock-out or POLK F171A knock-in cells

The targeting vectors were constructed by using the simple vector construction method based on the Multi Site Gateway® Technology (Life Technologies) as described [38]. For knock-out of *POLK*, genomic fragments were obtained by PCR amplification with Ex Taq Pol (Takara Bio) from Nalm-6 genomic DNA using primers KO-5armF (5′-GGGGACAACTTTGTATAGAAAAGTTGTGCTGTCTAAGAGACTGATAAT-3′) and KO-5armR (5′-GGGGACTGCTTTTTTGTACAAACTTGTAGCTACCTACTATATCTAGTTATAA-3′) for the 5′-arm, and KO-3armF (5′-GGGGACAGCTTTCTTGTACAAAGTGGTGACACAGAAGGGTTTGCTCAC-3′) and KO-3armR (5′-GGGGACAACTTTGTATAATAAAGTTGCAGGGTGGTCTCAAACTCCTG-3′) for the 3′-arm. The targeting vector was linearized with *Ahd*I and transfected into the Nalm-6 cells as described above. The targeted clones were confirmed by the Southern blotting analysis. For knock-in of *POLK F171A*, genomic fragments were obtained from Nalm-6 genomic DNA by PCR with KOD-FX (Toyobo) using primers KI-5armF (5′-GGGGACAACTTTGTATAGAAAAGTTGATGGTCTTGGTAACTTCCCTATGTTGC-3′) and KI-5armR (5′-GGGGACTGCTTTTTTGTACAAACTTGTGAGCCATCGCCATCGCACTC-3′) for the 5′-arm, and KI-3armF (5′-GGGGACAGCTTTCTTGTACAAAGTGGACCTTGCTCTACCTGGAGTTGGC-3′) and KI-3′armR (5′-GGGGACAACTTTGTATAATAAAGTTGTGCTCCCCTCTCCTCCACCAC-3′) for the 3′-arm. The mutation of TTT to GCT at codon 171, which directed an amino acid substitution of F171 to alanine, was introduced into the 3′-arm by PCR-mediated site-directed mutagenesis. The targeting vector was linearized with *Pme*I and transfected into $POLK^{+/-(Hygr)}$ cells. The targeting clones were confirmed by the genomic PCR using primers 5′-GAAGAGGTTCACTAGTACTGGCCATTGC-3′ and 5′-GCCAGAAGTTTTGCTGAGTTAAAGTACGACT-3′. Insertion of the puromycin-resistance gene (Pur^r) into the *POLK* wild-type allele in $POLK^{F171A/-(Hygr)}$ cell was confirmed by RT-PCR followed by sequencing analysis as described below and the genomic PCR using primers 5′-GATAATAATGGTTTCTTAGACGTCGCGGC-3′ and 5′-GAAGAGGTTCACTAGTACTGGCCATTGC-3′, which amplifies ~5 kb fragment when both $Puro^r$ and the hygromycin-resistance gene (Hyg^r) are targeted into the same *POLK* allele and no fragments are generated when $Puro^r$ and Hyg^r are targeted into the discrete *POLK* allele. The $Puro^r$ and the Hyg^r were removed by introduction of Cre recombinase expression vector by Nucleofector I.

2.3. Southern blot analysis

Southern blotting was performed as previously described [39]. Briefly, 10 μg of genomic DNA was digested with *Eco*RV, then subjected to electrophoresis in 0.8% agarose gel and the DNA was transferred onto a hybond-N^+ membrane (GE Healthcare Bio-Sciences),

followed by Southern hybridization with a ^{32}P-labeled probe that was obtained by PCR amplification from Nalm-6 genomic DNA using the following primers: 5′-CATCATGAGGACCCTGAACTATC-3′ and 5′-TCAGGT AGTCCACGAGCTTCG-3′.

2.4. Western blot analysis

Total cell extracts were prepared from exponentially growing cells and subjected to electrophoresis in 10% SDS-polyacrylamide gel and then electro-transferred onto a PVDF membrane (Millipore). The membrane was soaked with blocking buffer including 5% skim milk, then incubated with either polyclonal antibody against Pol κ or mouse anti-β-actin monoclonal antibody (Sigma–Aldrich), and finally incubated with peroxidase-conjugated anti-rabbit immunoglobulin or anti-mouse IgG conjugated to horseradish peroxidase (GE Healthcare Bio-Sciences). The polyclonal antibody was prepared by TaKaRa (Shiga, Japan) by immunization of a rabbit with purified C-terminally truncated 10 × HisTag human Pol κ_{1-559} [25]. The proteins were visualized by chemiluminescence using the ECL system (GE Healthcare Bio-Sciences).

2.5. RNA extraction and RT-PCR

Total RNA was extracted using RNeasy kit (Qiagen). For RT-PCR, total RNA was transcribed into cDNA using SuperScript III First-Strand Synthesis System (Invitrogen). The synthesized cDNA was used as the template for PCR using Ex Taq Pol (Takara Bio) with gene-specific primers 5′-GATAATAAAGCAGGGATGG-3′ and 5′-GCACTAGCTGTCAGTGTTGT-3′. The sequence of the *POLK*$^{F171A/-}$ cells were analyzed with 3130 Avant genetic analyzer (Applied Biosystems).

2.6. Construction of closed circular double-stranded plasmid DNA containing a single (−)- or (+)-BPDE-dG

The nucleotide position 123 of the *supF* gene was chosen for the (−)-BPDE-dG or (+)-BPDE-dG incorporation site because it has been recognized as a BPDE-induced mutational hotspot for G:C to T:A transversions [40]. The 21-mer oligodeoxynucleotide bearing BPDE-dG (5′-GCGGCCAAAGXGAGCAGACTC-3′, where X represent (−)-BPDE-dG or (+)-BPDE-dG) was synthesized as previously reported [41]. The pMY189 single-stranded DNA was prepared in *Escherichia coli* (*E. coli*) JM109 strain using VCSM13 helper phage as previously described [42]. The 5′-phosphorylated unmodified, (−)-BPDE-dG or (+)-BPDE-dG-modified oligodeoxynucleotide was annealed with pMY189 single-stranded DNA, and closed circular double-stranded DNA containing a single dG:dC, (−)-BPDE-dG:dC, or (+)-BPDE-dG:dC pair was synthesized and purified as previously described [43].

2.7. SupF forward mutation assay and sequencing analysis

Plasmid pMY189 with or without (−)-BPDE-dG or (+)-BPDE-dG (1 μg) was transfected into 2.0×10^6 cells by using Nucleofector I as described above. After 72 h of culturing in medium, propagated plasmids were extracted from the cells by the method described by Stary and Sarasin [44]. The recovered DNA was treated with *Dpn*I to digest unreplicated plasmids. The recovered plasmids were introduced into the KS40/pOF105 indicator bacteria [45] with a MicroPulser Electroporator (Bio-Rad Laboratories). To select *E. coli* with a mutated *supF* gene, the transformed cells were plated onto Luria-Bertani (LB) agar plates containing nalidixic acid (50 μg/ml), streptomycin (100 μg/ml), ampicillin (150 μg/ml), chloramphenicol (30 μg/ml), 5-bromo-4-chloro-3-indolyl-β-D-galactopyranoside (80 μg/ml), and isopropyl-β-D-thiogalactopyranoside (23.8 μg/ml). To determine the total number of transformants, the transformed cells were plated onto LB plates containing ampicillin (150 μg/ml) and chloramphenicol (30 μg/ml). The nucleotide sequences of the *supF* gene were analyzed by DNA sequencing, as previously described [46].

2.8. Statistical analysis

The statistical significance was examined using the Student's *t* test. Levels of $P < 0.05$ were considered significant.

3. Results

3.1. Establishment of *POLK*$^{+/-}$ and *POLK*$^{-/-}$ cells

POLK resides on chromosome 5 (coordinates 74.8–74.9 Mb of the human genome presented in Ensembl) and includes 15 exons. To disrupt the *POLK* gene in the human pre-B lymphoblastic leukemia cell line, Nalm-6, a targeting vector was constructed to delete exon 6 of the *POLK* gene, resulting in a frameshift (Fig. 1A). The targeting vectors have Hyg^r for the first targeting or Puro^r for the second targeting flanked by the *loxP* site and also contain the diphtherotoxin A (DT-A) gene to exclude random integrants. As a result of the first targeting, we obtained one heterozygous disrupted clone (*POLK*$^{+/-(Hygr)}$) out of 132 hygromycin-resistant clones. For the second targeting, the puromycin-resistance targeting vectors were transfected into the *POLK*$^{+/-(Hygr)}$ clone. We obtained one homo-disrupted clone (*POLK*$^{-(Puror)/-(Hygr)}$) out of 158 puromycin-resistant clones from *POLK*$^{+/-(Hygr)}$. The targeted disruption into the *POLK* gene was verified by Southern blot analysis using the *Eco*RV-digested genomic DNA with an external 3′ probe (Fig. 2A). To remove the Hyg^r and Puro^r cassettes from the resulting clones, the Cre expression vector was electroporated into the clones obtained above. The expression of the protein was then examined by Western blot analysis with anti-Pol κ antibody (Fig. 2B), which indicated that Pol κ protein was expressed in *POLK*$^{+/+}$ and *POLK*$^{+/-}$ cells, but not in *POLK*$^{-/-}$ cell. Loss of the expression of *POLK* mRNA in *POLK*$^{-/-}$ was confirmed by RT-PCR analysis (Fig. 2C). The doubling time of the *POLK*$^{+/-}$ (20.8 ± 0.59 h) or *POLK*$^{-/-}$ (20.9 ± 0.91 h) cell was similar to that of *POLK*$^{+/+}$ (20.2 ± 0.95 h) cell, showing that the knock-out of *POLK* does not significantly influence the proliferation rate of Nalm-6 cell line.

3.2. Establishment of *POLK*$^{F171A/-}$ cell

The knock-in cell that expresses *POLK* F171A (*POLK*$^{F171A/-}$) was generated from *POLK*$^{+/-(Hygr)}$ cells that possess a Hyg^r cassette in the *POLK* knock-out allele. The targeting vector was constructed to introduce the mutation (TTT to GCT) into exon 5 (Fig. 1B), resulting in the substitution of phenylalanine for alanine at codon 171. The targeting vector has a Puro^r cassette flanked by the *loxP* site and contains the DT-A gene. The targeting vector was linearized with *Pme*I and electroporated into the *POLK*$^{+/-(Hygr)}$ cell. After selecting the cells with puromycin, we obtained 7 positive clones, in which the Puro^r cassette was introduced into the targeted locus of *POLK* wild type or *POLK* knock-out allele, out of 133 puromycin-resistant clones. We further examined the expression of *POLK* mRNA and confirmed the sequence of the cDNA in clones (Fig. 2D). We obtained 2 clones that expressed the mutant *POLK* mRNA, i.e., *POLK* F171A, out of 7 clones, suggesting that the expected mutation was introduced into *POLK* wild-type allele in these clones. We also confirmed that the Puro^r cassette was introduced into the targeted locus of *POLK* wild type allele, but not *POLK* knock-out allele in these clones by genomic PCR (data not shown). The equivalent construct without the mutation was used to generate the mock-treated cell (*POLK*$^{mock/-}$). Puro^r and Hyg^r cassettes

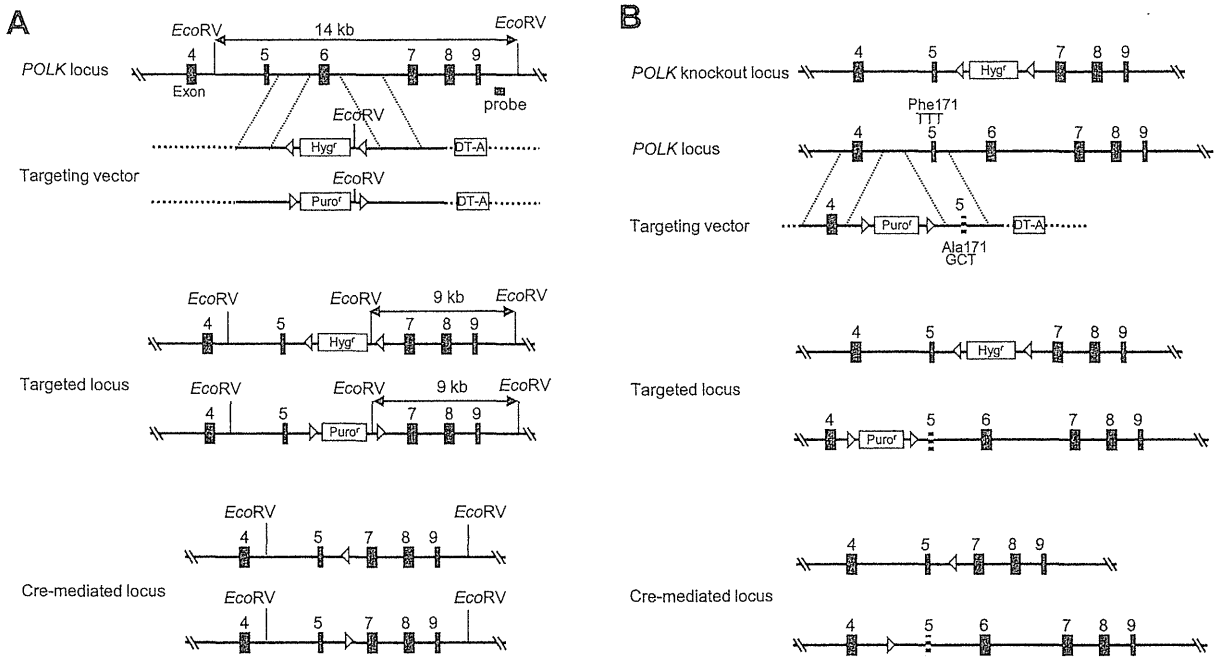

Fig. 1. Targeting strategy for generation of *POLK* mutant cells. Schematic representation of targeted disruption (A) and knock-in (B) of the *POLK* gene. The *POLK* locus, the targeting constructs, the targeted locus and the Cre-mediated locus are shown here. The black boxes, arrows and triangles represent exons, primers and *loxP* sequences, respectively. Phenylalanine 171 is coded in exon 5.

in the targeted alleles were removed by transient expression of Cre recombinase in the cells. The expression of Pol κ protein and mRNA in the established cells were confirmed by the Western blot analysis and RT-PCR (Fig. 2B and C). We confirmed no unintended mutations were introduced in exons 2, 3, 4 and 5 by DNA sequencing. The doubling time of $POLK^{F171A/-}$ (21.0 ± 0.71 h) and $POLK^{mock/-}$ (21.3 ± 0.49 h) cells were similar to that of $POLK^{+/-}$ cell as given above.

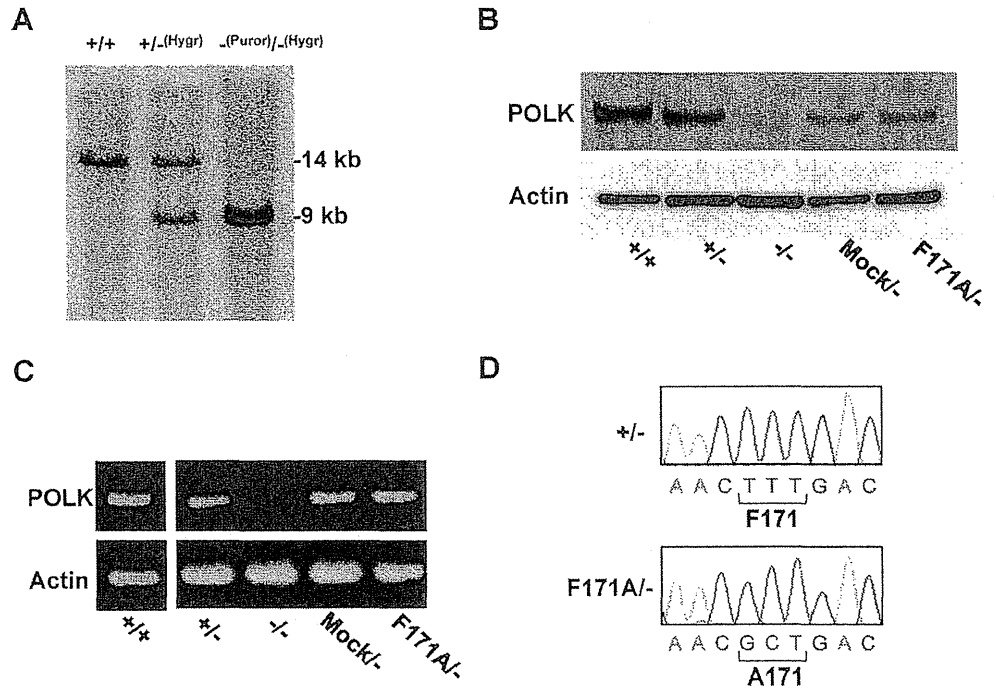

Fig. 2. Generation of $POLK^{+/-}$, $POLK^{-/-}$, and $POLK^{F171A/-}$ cells. (A) Southern blot analysis for *POLK* disruption. *Eco*RV-digested genomic DNA from wild-type (+/+), heterozygous (+/− (Hygr)), and homozygous (−(Puror)/−(Hygr)) *POLK* cells was loaded onto each lane. The probe used for the hybridization was indicated in Fig. 1. The wild-type allele (14 kb) and targeted alleles (9 kb) were indicated at right. (B) Western blot analysis for POLK protein. Whole cell extracts from $POLK^{+/+}$ $POLK^{+/-}$, $POLK^{-/-}$, $POLK^{mock/-}$, and $POLK^{F171A/-}$ cells were loaded onto a 10% of SDS-polyacrylamide gel. β-actin served as a loading control. (C) RT-PCR analysis for *POLK* mRNA. The same amounts of total RNA extracted from the each cell were used. β-actin served as an internal control. (D) Sequence of *POLK* cDNA generated by RT-PCR. The sequences around codon 171 were shown.

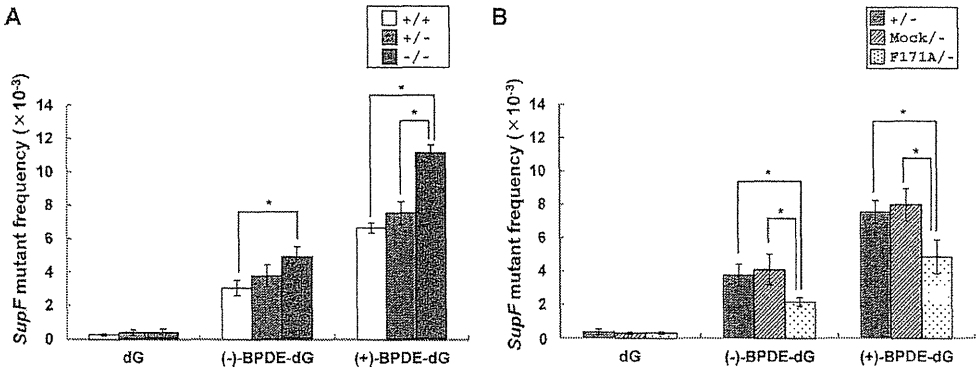

Fig. 3. Frequencies of the *supF* mutants induced by (−)- or (+)-*trans-anti*-BPDE-N^2-dG. Effect of (A) *POLK* disruption or (B) F171A knock-in on the mutant frequencies induced by dG:dC, (−)-*trans-anti*-BPDE-N^2-dG:dC, or (+)-*trans-anti*-BPDE-N^2-dG:dC pair. Data are expressed as mean ± standard deviation (SD) of 3 independent experiments. Asterisks indicate a significant difference with $P < 0.05$.

3.3. *Effect of knock-out or knock-in of POLK on the mutant frequencies induced by BPDE-dG*

Plasmid containing a single dG:dC, (−)-BPDE-dG:dC, or (+)-BPDE-dG:dC base-pair at position 123 of the *supF* gene was introduced and replicated in $POLK^{+/+}$, $POLK^{+/-}$, $POLK^{-/-}$, $POLK^{mock/-}$ or $POLK^{F171A/-}$ cells. Plasmids replicated in cells were recovered and introduced into the *E. coli* KS40/pOF105 indicator strain, in order to calculate the mutant frequencies for the *supF* gene [47].

We first examined the effect of the *POLK* knock-out on the mutagenesis induced by BPDE-dG adducts. As shown in Fig. 3A and Table S1, heterozygous and homozygous knock-out of *POLK* had no effect on the mutant frequency of the control plasmid containing dG:dC pair. In contrast, the mutant frequencies of the (−)-BPDE-dG:dC and (+)-BPDE-dG:dC pairs in $POLK^{+/-}$ cells (38×10^{-4} and 76×10^{-4}, respectively) were slightly higher than those in $POLK^{+/+}$ cells (31×10^{-4} and 67×10^{-4}, respectively), although the differences were not statistically significant. Furthermore, the mutant frequencies of these adducts were significantly increased in $POLK^{-/-}$ cells (49×10^{-4} and 112×10^{-4}, respectively) compared with those of $POLK^{+/+}$ cells, as consistent with the previous report [24].

Next, we examined the effect of the *POLK* F171A knock-in on the mutant frequencies of (−)- or (+)-BPDE-dG adducts in cells. Interestingly, the mutant frequencies of (−)-BPDE-dG:dC and (+)-BPDE-dG:dC pairs were significantly lower in $POLK^{F171A/-}$ cells (22×10^{-4} and 48×10^{-4}, respectively), as compared with $POLK^{+/-}$ (38×10^{-4} and 76×10^{-4}, respectively) and $POLK^{mock/-}$ cells (41×10^{-4} and 80×10^{-4}), respectively.

We further analyzed the mutation spectra induced by (−)-BPDE-dG:dC or (+)-BPDE-dG:dC pair in the *supF* gene in $POLK^{+/+}$, $POLK^{+/-}$, $POLK^{-/-}$, $POLK^{mock/-}$, or $POLK^{F171A/-}$ cells (Table 1). The most predominant mutation was G:C to T:A transversions at position 123 in all the cell lines. Lesser amount of G:C to C:G transversions, G:C to A:T transitions, one-base deletion, and tandem mutations at the adducted position were also observed. Neither knock-out of *POLK* nor knock-in of *POLK* F171A altered the mutation spectra induced by (−)-BPDE-dG:dC or (+)-BPDE-dG:dC.

4. Discussion

In the previous *in vitro* study, we revealed that F171A substitution of human Pol κ increases efficiency of dCMP incorporation opposite (−)- or (+)-BPDE-dG in DNA by 18 fold [35]. However, the k_{cat}/K_m values bypassing across the lesions by the wild-type Pol κ were 2–3 orders of magnitude smaller than those of incorporation of dCMP opposite normal dG. The small k_{cat}/K_m values for TLS across (−)- or (+)-BPDE-dG in DNA by the wild-type Pol κ have also been reported by other groups [19,23]. It was questioned, therefore, whether the increase in the k_{cat}/K_m value by the amino acid substitution *in vitro* has biological significance *in vivo*. To address the question, we established human cell lines expressing $POLK^{+/-}$, $POLK^{F171A/-}$, $POLK^{mock/-}$ and $POLK^{-/-}$ (KO) cells (Figs. 1 and 2) and examined the mutagenic sensitivities against plasmids carrying (−)- or (+)-BPDE-dG in the *supF* reporter gene. In the mutation assays, we employed a shuttle vector system, i.e., pMY189, to measure mutation frequencies induced by the specific DNA adduct although it is not very clear to what extent Pol κ behaves similarly in TLS in the plasmid and in the chromosome. (+)-BPDE-dG induced higher mutation frequencies than (−)-BPDE-dG regardless of the genotypes. These results are consistent with the previous results that (+)-BPDE-dG is more mutagenic than (−)-BPDE-dG [48,49]. Interestingly, the $POLK^{F171A/-}$ cells exhibited significantly lower frequencies of mutations induced by either (−)- or (+)-BPDE-dG compared to $POLK^{+/-}$ and $POLK^{mock/-}$ cells (Fig. 3). The spectrum of mutations induced by (−)- or (+)-BPDE-dG contained predominantly G:C to T:A at position 123 of the *supF* gene where the adducts were embedded regardless of the genotypes (Table 1). These results strongly suggest that the F171A derivative of Pol κ indeed continues DNA replication across (−)- and (+)-BPDE-dG in template DNA more efficiently than does the wild-type Pol κ in an error-free manner. It is formally possible that mutations are induced by the action of the F171A derivative of Pol κ because the derivative produces some errors during TLS across (−)- and (+)-BPDE-dG in template DNA *in vitro* [35]. However, we don't think this is the case because the derivative inserts dTMP in addition to dCMP opposite the adducts when one dNTP is present in the reaction mixture or induces one base deletions when four dNTPs are present in the mixture *in vitro*. These errors should lead to G:C to A:T transitions or one base deletions. As shown in Table 1, the predominant mutation observed in the cells expressing the F171A derivative was G:C to T:A transversions. In addition, the mutation spectra were not substantially different regardless of the status of Pol κ. Therefore, the mutations are generated by error-prone Pol(s) that inserts dAMP opposite the DNA adducts, not by the F171A derivative of Pol κ. Pol κ interacts with other proteins such as PCNA and REV1 *in vivo* [6]. These interactions may substantially enhance the efficiency of TLS by Pol κ, and thus the Pol may exhibit significant effects on TLS *in vivo* despite the small k_{cat}/K_m values *in vitro*.

Based on the current and previous results [35], along with the molecular dynamic studies [50] and the structure studies with the ternary complex of Pol κ [36], we conclude that F171 is a molecular brake for TLS across (−)- and (+)-BPDE-dG, in DNA by Pol κ. We speculate that F171 may flexibly rotate and interact with pyrene rings of both (−)- and (+)-BPDE-dG. Because F171A substitution

Table 1
Mutation spectra in *supF* induced by (−)- or (+)-*trans-anti*-BPDE-N^2-dG:dC in wild type, +/−, −/−, Mock/−, and F171A/− mutant cells.

Adduct[a]	Mutation	+/+	+/−	−/−	Mock/−	F171A/−
(−)-BPDE-dG	Single base substitution at site of adduct					
	^{123}G:C→T:A[b]	23 (62)[c]	47 (65)	45 (68)	24 (65)	22 (61)
	^{123}G:C→C:G	2 (5)	12 (17)	12 (18)	6 (16)	5 (14)
	^{123}G:C→A:T	7 (19)	11 (15)	6 (9)	7 (19)	9 (25)
	One base deletion at site of adduct					
	G^{123}GG→G-G[d]	0 (0)	1 (1)	0 (0)	0 (0)	0 (0)
	Tandem mutation at site of adduct					
	G^{123}GG→TTG	3 (8)	0 (0)	2 (3)	0 (0)	0 (0)
	G^{123}GG→−AG	2 (5)	0 (0)	0 (0)	0 (0)	0 (0)
	G^{123}GG→−TG	0 (0)	0 (0)	1 (2)	0 (0)	0 (0)
	Other	0 (0)	1 (1)	0 (0)	0 (0)	0 (0)
	Total	37 (100)	72 (100)	66 (100)	37 (100)	36 (100)
(+)-BPDE-dG	Single base substitution at site of adduct					
	^{123}G:C→T:A	34 (85)	66 (84)	59 (77)	33 (83)	30 (81)
	^{123}G:C→C:G	3 (8)	6 (8)	9 (12)	6 (15)	3 (8)
	^{123}G:C→A:T	1 (3)	5 (6)	2 (3)	0 (0)	2 (5)
	One base deletion at site of adduct					
	G^{123}GG→G-G	0 (0)	0 (0)	2 (3)	0 (0)	0 (0)
	Tandem mutation at site of adduct					
	G^{123}GG→TTG	2 (5)	1 (1)	3 (4)	1 (3)	1 (3)
	G^{123}GG→−TG	0 (0)	0 (0)	1 (1)	0 (0)	0 (0)
	G^{123}GG→GGGGGG	0 (0)	0 (0)	0 (0)	0 (0)	1 (3)
	Other	0 (0)	0 (0)	1 (1)	0 (0)	0 (0)
	Total	40 (100)	78 (100)	77 (100)	40 (100)	37 (100)

[a] (−)-BPDE-dG and (+)-BPDE-dG indicate (−)-*trans-anti*-BPDE-N^2-dG and (+)-*trans-anti*-BPDE-N^2-dG, respectively.
[b] ^{123}G indicates the position 123 in the *supF* gene.
[c] Numbers in parentheses represent the percentage of total number of mutants.
[d] "−" Indicates one-base deletion.

enhanced the error-free TLS across both lesions *in vitro* and *in vivo*, the interactions might interfere with correct Watson-Crick base-pairing between the modified dG and the incoming dCMP in the catalytic center of Pol κ. In general, the active sites of the Y-family Pols are more spacious than those of replicative Pols, allowing the accommodation of bulky adducts on the template bases [6]. The substitution of F171A could provide wider space in the active site, which enables Pol κ to more smoothly accommodate the lesion and continue DNA replication past the modified dG. In the previous study, we revealed that F171A substitution does not affect the fidelity of DNA replication across the lesions nor either the efficiency of dCMP incorporation opposite normal dG [35]. Thus, we suggest that the overall structure of Pol κ is not substantially affected by the amino acid substitution. There should be multiple Pols that compete with the primer DNA when replicative Pols are stalled at the lesions [6]. Due to the increased k_{cat}/K_m values incorporating dCMP opposite (−)- and (+)-BPDE-dG in DNA, the F171A derivative of Pol κ may become predominant over error-prone Pols, such as Pol ζ, thereby reducing the mutation frequencies. It is interesting that a variant form of TLS Pol has higher efficiency to continue DNA synthesis across the damage than the native form.

The conclusion that F171 is a molecular brake for DNA synthesis across BPDE adducts in DNA suggests that Pol κ is not well-tuned to bypass the adducts. Previous reports suggest that the cognate substrates for Pol κ may be BP adducts in DNA because the promoter region contains arylhydrocarbon receptor binding sites [51], and the mouse embryonic fibroblasts from *Polk*$^{-/-}$ mice exhibit hypersensitivity both to the killing effects of racemic-(±)-BPDE [34], and the mutagenic and lethal effects of BP plus rat liver homogenate (S9) in the presence of caffeine [33]. On the other hand, however, Pol κ binds only weakly to template/primer DNA containing (+)-BPDE adduct [25], which is the major DNA adduct induced by BPDE. Rather, it binds strongly to template/primer DNA containing (−)-BPDE adduct [25], which is a minor DNA adduct formed upon metabolic activation of BP. In addition, Pol κ more efficiently bypasses the (−)- adduct than the (+)-adduct [25]. These results along with the current *in vivo* results strongly suggest that Pol κ has not evolved to protect cells from BP or the related arylhydrocarbon carcinogens. This Pol is known to bypass other lesions induced by endogenous mutagens, i.e., methyl glyoxal [52], estrogen [53] and reactive oxygen species [54]. *Polk*$^{-/-}$ mice exhibit increased spontaneous mutations in the liver, kidney and lung, but not in testis, in older animals [34] and the mutation frequencies are enhanced by dietary cholesterol [55]. These results further suggest that the cognate lesion is the one induced by endogenous mutagens, which may increase the lesion in the organs during the aging process. These results may also explain why *POLK*$^{-/-}$ cells did not exhibit slow growth and high spontaneous mutation frequencies in this study. The cognate lesion might not be effectively induced in cultured cells.

In the current study, we took advantage of human Nalm-6 cells to engineer cell lines expressing a variant form of Pol κ. Unlike other human cell lines, which exhibit poor gene targeting efficiency, this cell line displays 1–30% gene targeting efficiencies [56]. In fact, we obtained one *POLK*$^{+/-}$ cell out of 132 wild-type cells (=0.8%) and one *POLK*$^{-/-}$ cell out of 158 *POLK*$^{+/-}$ cells (=0.6%). For the knock-in mutants, we obtained 2 *POLK*$^{F171A/-}$ cells out of 133 *POLK*$^{+/-}$ cells (=1.5%). Currently, gene knockdown with siRNA is the common technique to suppress gene expression in human cells because of the difficulty in obtaining such gene knock-out and knock-in cells. However, gene knockdown only reduces the expression by about 80% and does not completely shut it down. Embryonic fibroblasts from knock-out mice are an alternative available experimental resource by which to examine gene functions in mammals. Nevertheless, it is pointed out that the mouse cells do not exhibit similar TLS efficiency or accuracy compared to those of human cells [57]. Therefore, we believe that Nalm-6 cells are useful for genetic analyses of human genes including those involved in DNA repair and mutagenesis.

In summary, we established a human cell line expressing an F171 variant of Pol κ and suggest that this residue is used by Pol κ as a molecular brake for TLS across (−)- and (+)-BPDE-dG in DNA. The presence of such a brake in the active site raises a possibility that Pol κ has not evolved to protect cells from BP. Thus a complete

understanding of the role of Pol κ in protecting cells against the mutagenic and carcinogenic effects of endogenous mutagens is still lacking, and further investigations, both *in vitro* and *in vivo*, are needed.

Conflict of interest

We have no competing interests or conflicts of interest concerning the research presented in this paper.

Acknowledgments

This work was supported by grants-in-aid for scientific research from the Ministry of Education, Culture, Sports, Science and Technology, Japan (MEXT, 18201010; MEXT, 22241016), the Ministry of Health, Labour and Welfare, Japan (MHLW, H21-Food-General-009), and the Japan Health Science Foundation (KHB1007); for cancer research from MHLW (20 designated-8); the Food Safety Commission.

Appendix A. Supplementary data

Supplementary data associated with this article can be found, in the online version, at http://dx.doi.org/10.1016/j.dnarep.2013.12.008.

References

[1] E.C. Friedberg, R. Wagner, M. Radman, Specialized DNA polymerases, cellular survival, and the genesis of mutations, Science 296 (2002) 1627–1630.
[2] T. Nohmi, Environmental stress and lesion-bypass DNA polymerases, Annu. Rev. Microbiol. 60 (2006) 231–253.
[3] P.M. Burgers, E.V. Koonin, E. Bruford, L. Blanco, K.C. Burtis, M.F. Christman, W.C. Copeland, E.C. Friedberg, F. Hanaoka, D.C. Hinkle, C.W. Lawrence, M. Nakanishi, H. Ohmori, L. Prakash, S. Prakash, C.A. Reynaud, A. Sugino, T. Todo, Z. Wang, J.C. Weill, R. Woodgate, Eukaryotic DNA polymerases: proposal for a revised nomenclature, J. Biol. Chem. 276 (2001) 43487–43490.
[4] S. Prakash, R.E. Johnson, L. Prakash, Eukaryotic translesion synthesis DNA polymerases: specificity of structure and function, Annu. Rev. Biochem. 74 (2005) 317–353.
[5] S.S. Lange, K. Takata, R.D. Wood, DNA polymerases and cancer, Nat. Rev. Cancer 11 (2011) 96–110.
[6] J.E. Sale, A.R. Lehmann, R. Woodgate, Y-family DNA polymerases and their role in tolerance of cellular DNA damage, Nat. Rev. Mol. Cell Biol. 13 (2012) 141–152.
[7] C. Masutani, R. Kusumoto, A. Yamada, N. Dohmae, M. Yokoi, M. Yuasa, M. Araki, S. Iwai, K. Takio, F. Hanaoka, The *XPV* (xeroderma pigmentosum variant) gene encodes human DNA polymerase eta, Nature 399 (1999) 700–704.
[8] R.E. Johnson, C.M. Kondratick, S. Prakash, L. Prakash, hRAD30 mutations in the variant form of xeroderma pigmentosum, Science 285 (1999) 263–265.
[9] A.J. Rattray, J.N. Strathern, Error-prone DNA polymerases: when making a mistake is the only way to get ahead, Annu. Rev. Genet. 37 (2003) 31–66.
[10] K. Bebenek, T.A. Kunkel, Functions of DNA polymerases, Adv. Protein Chem. 69 (2004) 137–165.
[11] M.F. Goodman, Error-prone repair DNA polymerases in prokaryotes and eukaryotes, Annu. Rev. Biochem. 71 (2002) 17–50.
[12] H. Ling, F. Boudsocq, R. Woodgate, W. Yang, Snapshots of replication through an abasic lesion; structural basis for base substitutions and frameshifts, Mol. Cell 13 (2004) 751–762.
[13] V.L. Gerlach, W.J. Feaver, P.L. Fischhaber, E.C. Friedberg, Purification and characterization of pol kappa, a DNA polymerase encoded by the human *DINB1* gene, J. Biol. Chem. 276 (2001) 92–98.
[14] T. Ogi, T. Kato Jr., T. Kato, H. Ohmori, Mutation enhancement by DINB1, a mammalian homologue of the *Escherichia coli* mutagenesis protein *dinB*, Genes Cells 4 (1999) 607–618.
[15] R.E. Johnson, S. Prakash, L. Prakash, The human *DINB1* gene encodes the DNA polymerase Pol θ, Proc. Natl. Acad. Sci. U. S. A 97 (2000) 3838–3843.
[16] H. Ohmori, E.C. Friedberg, R.P. Fuchs, M.F. Goodman, F. Hanaoka, D. Hinkle, T.A. Kunkel, C.W. Lawrence, Z. Livneh, T. Nohmi, L. Prakash, S. Prakash, T. Todo, G.C. Walker, Z. Wang, R. Woodgate, The Y-family of DNA polymerases, Mol. Cell 8 (2001) 7–8.
[17] J. Wagner, P. Gruz, S.R. Kim, M. Yamada, K. Matsui, R.P. Fuchs, T. Nohmi, The *dinB* gene encodes a novel *E. coli* DNA polymerase, DNA pol IV, involved in mutagenesis, Mol. Cell 4 (1999) 281–286.
[18] P. Gruz, F.M. Pisani, M. Shimizu, M. Yamada, I. Hayashi, K. Morikawa, T. Nohmi, Synthetic activity of Sso DNA polymerase Y1, an archaeal DinB-like DNA polymerase, is stimulated by processivity factors proliferating cell nuclear antigen and replication factor C, J. Biol. Chem. 276 (2001) 47394–47401.
[19] N. Suzuki, E. Ohashi, A. Kolbanovskiy, N.E. Geacintov, A.P. Grollman, H. Ohmori, S. Shibutani, Translesion synthesis by human DNA polymeraseκ on a DNA template containing a single stereoisomer of dG-(+)- or dG-(-)-*anti*-N^2-BPDE (7 8-dihydroxy-anti-9,10-epoxy-7,8,9,10-tetrahydrobenzo[a]pyrene), Biochemistry 41 (2002) 6100–6106.
[20] Y. Zhang, F. Yuan, X. Wu, M. Wang, O. Rechkoblit, J.S. Taylor, N.E. Geacintov, Z. Wang, Error-free and error-prone lesion bypass by human DNA polymerase κ *in vitro*, Nucleic Acids Res. 28 (2000) 4138–4146.
[21] O. Rechkoblit, Y. Zhang, D. Guo, Z. Wang, S. Amin, J. Krzeminsky, N. Louneva, N.E. Geacintov, Translesion synthesis past bulky benzo[a]pyrene diol epoxide N^2-dG and N^6-dA lesions catalyzed by DNA bypass polymerases, J. Biol. Chem. 277 (2002) 30488–30494.
[22] J.Y. Choi, K.C. Angel, F.P. Guengerich, Translesion synthesis across bulky N^2-alkyl guanine DNA adducts by human DNA polymerase κ, J. Biol. Chem. 281 (2006) 21062–21072.
[23] X. Huang, A. Kolbanovskiy, X. Wu, Y. Zhang, Z. Wang, P. Zhuang, S. Amin, N.E. Geacintov, Effects of base sequence context on translesion synthesis past a bulky (+)-*trans-anti*-B[a]P-N^2-dG lesion catalyzed by the Y-family polymerase pol κ, Biochemistry 42 (2003) 2456–2466.
[24] S. Avkin, M. Goldsmith, S. Velasco-Miguel, N. Geacintov, E.C. Friedberg, Z. Livneh, Quantitative analysis of translesion DNA synthesis across a benzo[a]pyrene-guanine adduct in mammalian cells: the role of DNA polymerase kappa, J. Biol. Chem. 279 (2004) 53298–53305.
[25] N. Niimi, A. Sassa, A. Katafuchi, P. Gruz, H. Fujimoto, R.R. Bonala, F. Johnson, T. Ohta, T. Nohmi, The steric gate amino acid tyrosine 112 is required for efficient mismatched-primer extension by human DNA polymerase kappa, Biochemistry 48 (2009) 4239–4246.
[26] H. Fukuda, T. Takamura-Enya, Y. Masuda, T. Nohmi, C. Seki, K. Kamiya, T. Sugimura, C. Masutani, F. Hanaoka, H. Nakagama, Translesional DNA synthesis through a C8-guanyl adduct of 2-amino-1-methyl-6-phenylimidazo[4 5-b]pyridine (PhIP) in Vitro: Rev1 inserts dc opposite the lesion and DNA polymerase kappa potentially catalyzes extension reaction from the 3'-dC terminus, J. Biol. Chem. (2009).
[27] P.L. Fischhaber, V.L. Gerlach, W.J. Feaver, Z. Hatahet, S.S. Wallace, E.C. Friedberg, Human DNA polymerase κ bypasses and extends beyond thymine glycols during translesion synthesis *in vitro*, preferentially incorporating correct nucleotides, J. Biol. Chem. 277 (2002) 37604–37611.
[28] P. Jaloszynski, E. Ohashi, H. Ohmori, S. Nishimura, Error-prone and inefficient replication across 8-hydroxyguanine (8-oxoguanine) in human and mouse ras gene fragments by DNA polymerase kappa, Genes Cells 10 (2005) 543–550.
[29] I.G. Minko, M.B. Harbut, I.D. Kozekov, A. Kozekova, P.M. Jakobs, S.B. Olson, R.E. Moses, T.M. Harris, C.J. Rizzo, R.S. Lloyd, Role for DNA polymerase kappa in the processing of N^2-N^2-guanine interstrand cross-links, J. Biol. Chem. 283 (2008) 17075–17082.
[30] D.H. Phillips, P.L. Grover, Polycyclic hydrocarbon activation: bay regions and beyond, Drug Metab. Rev. 26 (1994) 443–467.
[31] K. Peltonen, A. Dipple, Polycyclic aromatic hydrocarbons: chemistry of DNA adduct formation, J. Occup. Environ. Med. 37 (1995) 52–58.
[32] Y. Zhang, X. Wu, D. Guo, O. Rechkoblit, N.E. Geacintov, Z. Wang, Two-step error-prone bypass of the (+)- and (-)-*trans-anti*-BPDE-N^2-dG adducts by human DNA polymerases eta and kappa, Mutat. Res. 510 (2002) 23–35.
[33] T. Ogi, Y. Shinkai, K. Tanaka, H. Ohmori, Polκ protects mammalian cells against the lethal and mutagenic effects of benzo[a]pyrene, Proc. Natl. Acad. Sci. U. S. A 99 (2002) 15548–15553.
[34] J.N. Stancel, L.D. McDaniel, S. Velasco, J. Richardson, C. Guo, E.C. Friedberg, *Polk* mutant mice have a spontaneous mutator phenotype, DNA Rep. (Amst) 8 (2009) 1355–1362.
[35] A. Sassa, N. Niimi, H. Fujimoto, A. Katafuchi, P. Gruz, M. Yasui, R.C. Gupta, F. Johnson, T. Ohta, T. Nohmi, Phenylalanine 171 is a molecular brake for translesion synthesis across benzo[a]pyrene-guanine adducts by human DNA polymerase kappa, Mutat. Res. 718 (2011) 10–17.
[36] S. Lone, S.A. Townson, S.N. Uljon, R.E. Johnson, A. Brahma, D.T. Nair, S. Prakash, L. Prakash, A.K. Aggarwal, Human DNA polymerase κ encircles DNA: implications for mismatch extension and lesion bypass, Mol. Cell 25 (2007) 601–614.
[37] T. Suzuki, A. Ukai, M. Honma, N. Adachi, T. Nohmi, Restoration of mismatch repair functions in human cell line Nalm-6, which has high efficiency for gene targeting, PLoS One 8 (2013) e61189.
[38] S. Iiizumi, Y. Nomura, S. So, K. Uegaki, K. Aoki, K. Shibahara, N. Adachi, H. Koyama, Simple one-week method to construct gene-targeting vectors: application to production of human knockout cell lines, Biotechniques 41 (2006) 311–316.
[39] S. So, N. Adachi, M.R. Lieber, H. Koyama, Genetic interactions between BLM and DNA ligase IV in human cells, J. Biol. Chem. 279 (2004) 55433–55442.
[40] J.L. Yang, V.M. Maher, J.J. McCormick, Kinds of mutations formed when a shuttle vector containing adducts of (+/-)-7β 8α-dihydroxy-9α, 10α-epoxy-7,8,9, 10-tetrahydrobenzo[a]pyrene replicates in human cells, Proc. Natl. Acad. Sci. U. S. A 84 (1987) 3787–3791.
[41] F. Johnson, R. Bonala, D. Tawde, M.C. Torres, C.R. Iden, Efficient synthesis of the benzo[a]pyrene metabolic adducts of 2'-deoxyguanosine and 2'-deoxyadenosine and their direct incorporation into DNA, Chem. Res. Toxicol. 15 (2002) 1489–1494.
[42] H. Kamiya, H. Kasai, 2-Hydroxy-dATP is incorporated opposite G by Escherichia coli DNA polymerase III resulting in high mutagenicity, Nucleic Acids Res. 28 (2000) 1640–1646.

[43] N. Sunaga, T. Kohno, K. Shinmura, T. Saitoh, T. Matsuda, R. Saito, J. Yokota, OGG1 protein suppresses G:C → T:A mutation in a shuttle vector containing 8-hydroxyguanine in human cells, Carcinogenesis 22 (2001) 1355–1362.
[44] A. Stary, A. Sarasin, Simian virus 40 (SV40) large T antigen-dependent amplification of an Epstein-Barr virus-SV40 hybrid shuttle vector integrated into the human HeLa cell genome, J. Gen. Virol. 73 (Pt 7) (1992) 1679–1685.
[45] F. Obata, T. Nunoshiba, T. Hashimoto-Gotoh, K. Yamamoto, An improved system for selection of forward mutations in an *Escherichia coli supF* gene carried by plasmids, J. Radiat. Res. 39 (1998) 263–270.
[46] N. Murata-Kamiya, H. Kamiya, H. Kaji, H. Kasai, Glyoxal, a major product of DNA oxidation, induces mutations at G:C sites on a shuttle vector plasmid replicated in mammalian cells, Nucleic Acids Res. 25 (1997) 1897–1902.
[47] T. Yagi, The achievement of shuttle vector techniques in mammalian mutation research, Genes Environ. 35 (2013) 93–98.
[48] M. Moriya, S. Spiegel, A. Fernandes, S. Amin, T. Liu, N. Geacintov, A.P. Grollman, Fidelity of translesional synthesis past benzo[a]pyrene diol epoxide-2′-deoxyguanosine DNA adducts: marked effects of host cell, sequence context, and chirality, Biochemistry 35 (1996) 16646–16651.
[49] P. Brookes, M.R. Osborne, Mutation in mammalian cells by stereoisomers of anti-benzo[a]pyrene-diolepoxide in relation to the extent and nature of the DNA reaction products, Carcinogenesis 3 (1982) 1223–1226.
[50] L. Jia, N.E. Geacintov, S. Broyde, The N-clasp of human DNA polymerase kappa promotes blockage or error-free bypass of adenine- or guanine-benzo[a]pyrenyl lesions, Nucleic Acids Res. 36 (2008) 6571–6584.
[51] T. Ogi, J. Mimura, M. Hikida, H. Fujimoto, Y. Fujii-Kuriyama, H. Ohmori, Expression of human and mouse genes encoding polκ: testis-specific developmental regulation and AhR-dependent inducible transcription, Genes Cells 6 (2001) 943–953.
[52] B. Yuan, C. You, N. Andersen, Y. Jiang, M. Moriya, T.R. O'Connor, Y. Wang, The roles of DNA polymerases kappa and iota in the error-free bypass of N2-carboxyalkyl-2′-deoxyguanosine lesions in mammalian cells, J. Biol. Chem. 286 (2011) 17503–17511.
[53] A. Mizutani, T. Okada, S. Shibutani, E. Sonoda, H. Hochegger, C. Nishigori, Y. Miyachi, S. Takeda, M. Yamazoe, Extensive chromosomal breaks are induced by tamoxifen and estrogen in DNA repair-deficient cells, Cancer Res. 64 (2004) 3144–3147.
[54] J.H. Yoon, G. Bhatia, S. Prakash, L. Prakash, Error-free replicative bypass of thymine glycol by the combined action of DNA polymerases kappa and zeta in human cells, Proc. Natl. Acad. Sci. U. S. A 107 (2010) 14112–14116.
[55] W.D. Singer, L.C. Osimiri, E.C. Friedberg, Increased dietary cholesterol promotes enhanced mutagenesis in DNA polymerase kappa-deficient mice, DNA Rep. (Amst) 12 (2013) 817–823.
[56] N. Adachi, S. So, S. Iiizumi, Y. Nomura, K. Murai, C. Yamakawa, K. Miyagawa, H. Koyama, The human pre-B cell line Nalm-6 is highly proficient in gene targeting by homologous recombination, DNA Cell Biol. 25 (2006) 19–24.
[57] S. Shachar, O. Ziv, S. Avkin, S. Adar, J. Wittschieben, T. Reissner, S. Chaney, E.C. Friedberg, Z. Wang, T. Carell, N. Geacintov, Z. Livneh, Two-polymerase mechanisms dictate error-free and error-prone translesion DNA synthesis in mammals, EMBO J. 28 (2009) 383–393.

DNA Repair 15 (2014) 11–20

Contents lists available at ScienceDirect

DNA Repair

journal homepage: www.elsevier.com/locate/dnarepair

Tracing the fates of site-specifically introduced DNA adducts in the human genome☆

Manabu Yasui[a,*], Yuki Kanemaru[a], Nagisa Kamoshita[a], Tetsuya Suzuki[a], Toshiya Arakawa[b], Masamitsu Honma[a,**]

[a] Division of Genetics and Mutagenesis, National Institute of Health Sciences, 1-18-1 Kamiyoga, Setagaya-ku, Tokyo 158-8501, Japan
[b] Department of Biochemistry, School of Dentistry, Health Sciences University of Hokkaido, Tobetsu-cho, Hokkaido 061-0293, Japan

ARTICLE INFO

Article history:
Received 20 August 2013
Received in revised form 9 January 2014
Accepted 15 January 2014

Keywords:
DNA adducts
Mutagenesis
Gene targeting
8-Oxoguanine (8-oxoG)

ABSTRACT

We developed a system for tracing DNA adducts in targeted mutagenesis (TATAM) and investigated the prevalence and types of consequent mutations. Targeted mutagenesis methods site-specifically replace endogenous DNA bases with bases carrying synthetic adducts using targeting vectors. The TATAM system was enabled by introduction of site-specific DNA double strand breaks (DSB), which strongly enhanced targeting efficiency through homologous recombination (HR), and a new polymerase chain reaction-based technique, which gives high yields of the target vectors carrying DNA adducts. Human lymphoblastoid TSCER122 cells are compound heterozygous for the thymidine kinase gene (*TK*−/−), and have a homing endonuclease I-*Sce*I site in intron 4 of the *TK* gene. The TATAM system enabled targeting of the *TK*− allele with the I-*Sce*I site using a synthetic *TK*+ allele containing an 8-oxo-7,8-dihydroguanine (8-oxoG) adduct, a typical product of oxidative DNA damage. The targeted clones (*TK*+/−) were then isolated by drug selection. Site-specific HR for DSB induced by I-SceI improved targeted integration of the synthetic allele by five orders of magnitude (from 10^{-7} to 10^{-2}). Subsequent analyses of approximately 800 target clones revealed that 8-oxoG was restored to G in 86% clones, probably reflecting base excision repair or translesion synthesis without mutation. Lesions of the remaining clones (14%) were associated with mutations. The mutation spectrum corresponded closely with that of oxidative DNA damage inducers reported, in which G:C to T:A transversions (5.9%) were predominant. Over-expression of MutY homologs in cells, which prevents G:C to T:A transversions by removing 8-oxoG:A mispairing, significantly decreased the frequency of mutations to 2.6%, indicating that the 8-oxoG adducts introduced by the TATAM system are processed in the same manner as those generated by oxidative DNA damage.

1. Introduction

Humans are frequently exposed to thousands of potentially harmful dietary and environmental chemicals, many of which bind DNA and produce DNA adducts [1,2]. Furthermore, numerous known and unknown DNA adducts are constitutively present in human genomes, indicating exposure to DNA-reactive agents [3,4]. Owing to apoptotic and DNA repair mechanisms that eliminate premutagenic cells, not all DNA adducts lead to mutations [5–8]. However, numerous known mutagenic DNA-reactive agents produce specific gene mutations that are potentially carcinogenic.

Although relationships between specific DNA adducts and their characteristic mutagenic properties have been established, that between specific DNA adducts and mutations remain elusive. Indeed, multiple DNA adducts are often produced by single mutagens such as aflatoxin B1 and it remains unknown which of these are associated with major mutational events [9–11]. Studies of site-specific mutagenesis, DNA repair, and bypass using site-specifically modified oligonucleotides to monitor the fate of a DNA adduct induced by chemicals and radiation have been reviewed [9]. Numerous studies have employed extra-chromosomal approaches with episomal vectors, in which adduct-modified oligodeoxynucleotides are ligated into single- or double-stranded vectors

Abbreviations: TATAM, tracing DNA adducts in targeted mutagenesis; 8-oxoG, 8-oxo-7,8-dihydroguanine; *TK*, thymidine kinase gene; HR, homologous recombination; DSB, double-strand break; MYH, human MutY homolog.

* Corresponding author. Tel.: +81 3 3700 1141x434; fax: +81 3 3700 2348.
** Corresponding author. Tel.: +81 3 3700 9872; fax: +81 3 3700 2348.
E-mail addresses: m-yasui@nihs.go.jp (M. Yasui), honma@nihs.go.jp (M. Honma).

http://dx.doi.org/10.1016/j.dnarep.2014.01.003

containing replication origins and are transfected into cells [9,12–17]. These episomal vectors independently replicate from the host genome. However, DNA adducts may be processed *via* different mechanisms to those occurring in the genome. To demonstrate direct association between DNA adducts and genomic mutations, DNA adducts must be directly introduced into host genomes for subsequent investigations of their effects.

Site-specific intra-chromosomal mutagenesis was first reported by Essigmann and colleagues [18,19]. In these studies, SV40 vectors containing single adducts were randomly integrated into the genomes of Chinese hamster ovary cells. Subsequently, clones were isolated by drug selection, and the DNA at the adduct sites was sequenced. In a more recent study, Izhar et al. developed a unique system using phage integrase-mediated integration of plasmid-borne synthetic DNA adducts with defined site-specific DNA lesions into mammalian genomes [20]. This unique system demonstrated the genetic consequences of the 6-4 photoproduct and benzo[a]pyrene-guanine adduct after processing of translesion DNA synthesis (TLS) and homology-dependent repair in the human genome.

We previously developed a system for tracing the genetic consequences of DNA double strand breaks (DSBs) by introducing the homing endonuclease I-*Sce*I site into intron 4 of the thymidine kinase gene (*TK*) in human lymphoblastoid TK6 cells [21–23]. These experiments showed that the I-SceI-inducing DSB significantly enhanced homologous recombination (HR). In the present study, we developed a unique system for tracing DNA adducts in targeted mutagenesis (TATAM) that can site-specifically replace endogenous DNA bases in intron 4 of *TK* gene with bases containing a synthetic DNA adducts (Fig. 1). Subsequently, we traced the genetic consequences of the integrated DNA adduct. DSB enabled high gene targeting efficiency for the TATAM system following enhanced site-specific HR for DSB repair [24,25]. Using the TATAM system, we also stably introduced an 8-oxo-7,8-dihydroguanine (8-oxoG) adduct, which is a typical product of oxygen radical-forming agents, into non-transcribed (NTS) and transcribed strands (TS) of *TK* gene at high frequency. This is the first report to trace the fate of a DNA adduct occurring in an endogenous single-copy gene in the human genome.

2. Materials and methods

2.1. Cell culture

Cells were cultured in RPMI 1640 medium (Nacalai Tesque Corp., Kyoto, Japan) supplemented with 10% heat-inactivated horse serum (JRH Biosciences, Lenexa, KS, USA), 200 μg/ml sodium pyruvate, 100 U/ml penicillin, and 100 μg/ml streptomycin, and 10^5–10^6 cells/ml were maintained at 37 °C in 5% CO_2 and 100% humidity.

2.2. Construction of TSCER122 cells

TSCER122 human lymphoblastoid cells were isolated from TSCE105 cells [22], which were derived from TK6 cells [26]. TSCE105 (*TK*+/−) cells are heterozygous for a point mutation in exon 4 of the *TK* gene and have two I-*Sce*I recognition sites surrounding exon 5 of the *TK* allele. The I-SceI expression vector pCBASce (50 μg) was transfected into TSCE105 (5×10^6) cells that were suspended in 0.1 ml of Nucleofector solution V (Amaxa Biosystem, Koeln, Germany) using Nucleofector I according to the manufacturer's recommendations [27]. Subsequently, cells were seeded into 96-microwell plates at 1 cell/well. Two weeks later, *TK*-deficient mutants (*TK*−/−) were isolated in the presence of 2.0 μg/ml trifluorothymidine (TFT). Mutants were independently expended and DNAs were analyzed. DSBs occurring at the two I-*Sce*I sites in TSCE105 cells were correctly fused by error-free end-joining, and produced a new I-*Sce*I site with a 356-bp deletion containing the entire exon 5. The resulting *TK*-deficient mutant TSCER122 (Fig. 3A) was confirmed by drug resistance, I-SceI digestion, and DNA sequencing experiments.

2.3. Construction of MYH-overexpressing TSCER122 cells

The coding region of the human *MutY* homolog gene (MYH) was amplified from cDNA of TK6 human lymphoblastoid cells using polymerase chain reaction (PCR) with the primers 5′-TGG GAA TTC GCC ACC ATG AGG AAG CCA CG-3′ and 5′-TTT CAG TCG ACT CAC TGG GCT GCA CTG TT-3′. PCR products were digested using *EcoRI*/*SalI* restriction enzymes and were cloned into the *EcoRI*/*SalI* site of the pCI-neo Mammalian Expression Vector (Promega Corp., Madison, WI). The resulting pCI-MYHβ3 contained variant beta 3, which is known to localize in the nucleus [28,29]. TSCER122 cells (5×10^6) were transfected with 10 μg *Xmn*I-linearized pCI-MYHβ3 using Nucleofector I, were cultured for 48 h, and were then seeded into 96-microwell plates in the presence of 0.6 mg/ml G418 (Sigma-Aldrich, St. Louis, MO, USA). G418-resistant clones were then isolated and MYH protein expression was quantified using western blotting analyses and ImageGauge software (Fujifilm, Tokyo, Japan). MYH protein expression was normalized to β-actin, and was compared to that in wild type cells.

2.4. PCR-based preparation of a site-specifically modified targeting vector containing a single 8-oxoG adduct

The targeting vector pvINT^{8OxG}, which contained a single 8-oxoG adduct, and the control vector pvINT^{G} were prepared as described previously [30]. In brief, the method involved the following: (i) primer design, (ii) PCR amplification, (iii) isolation and self-annealing of four single-stranded (ss) DNA fragments originating from four individual PCR amplicons, and (iv) T4 DNA ligation (Fig. 2A). The plasmid pTK15 (9-kb) was derived from pTK10 [21,22] and was used as a PCR template. This plasmid vector comprises 6.1-kb of the original *TK* gene, encompassing exons 5–7, and the part of I-*Sce*I sequence in intron 4, which carries a loss of function TTAT deletion. We inserted 8-oxoG into the pvINT^{8OxG} vector in place of the central guanine at the *Bss*SI site in the NTS (5′-CTCGTG in Primer 3F) of *TK* gene (Fig. 2B). Moreover, we labeled a 5′-TTCA-sequence (*MseI*^{R}) near the 8-oxoG-modified *Bss*SI site that was resistant to *Mse*I digestion, and thereby distinguished between targeted and non-targeted revertants according inter-allelic recombination (Fig. 3B). Twenty primers were designed to amplify sequential 300-bp fragments from the end of the 6.1-kbp targeting vector, and the whole sequence was analyzed using an ABI 3730xl 96-capillary DNA analyzer (Applied Biosystems, Foster City, CA, USA).

2.5. Transfection and cloning of TK revertant cells using the TATAM system

TSCER122 (5×10^6) cells were suspended in 0.1 ml Nucleofector Solution V and were co-transfected with 50 μg of pCBASce vector and 2 μg of targeting vector (pvINT^{8OxG} or pvINT^{G}) using Nucleofector I according to the manufacturer's recommendations [27]. Subsequently, cells were cultured for 72 h and were then seeded into 96-microwell plates in the presence of HAT (200 μM hypoxanthine, 0.1 μM aminopterin, and 17.5 μM thymidine) to isolate 8-oxoG-integrated revertant clones. Drug-resistant colonies were counted 2 weeks later, frequencies of *TK*

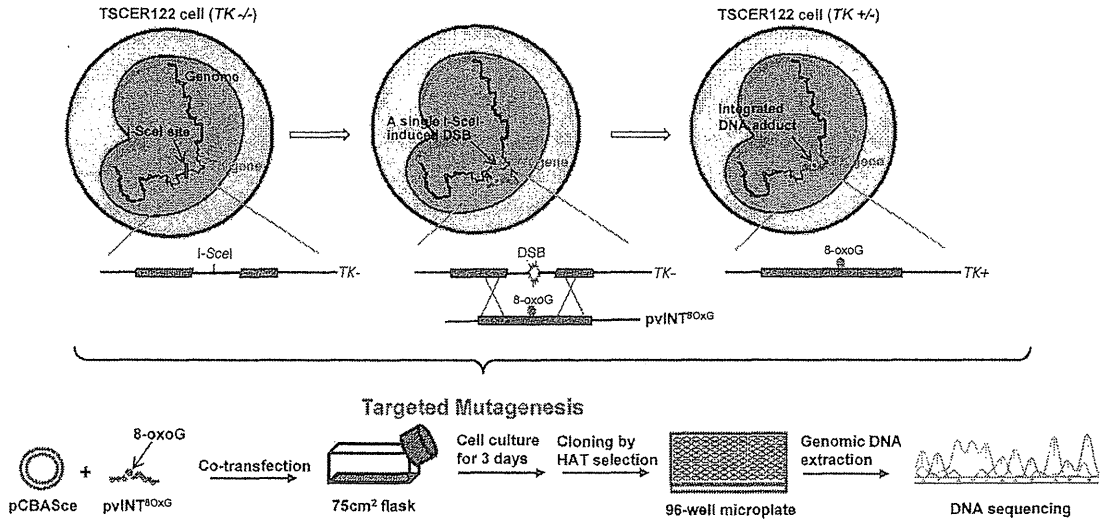

Fig. 1. Outline of the tracing DNA adducts in targeted mutagenesis (TATAM) system. The human lymphoblastoid cell line TSCER122 is compound heterozygous for thymidine kinase gene (*TK*−/−) and has a single I-*Sce*I endonuclease site. TSECR122 cells were co-transfected with the 8-oxoG-modified targeting vector pvINT^{8OxG} and the I-SceI expression plasmid pCBASce. Three days after transfection, cells were seeded into 96-microwell plates in the presence of HAT to isolate 8-oxoG-integrated *TK*-revertant clones. Subsequently, the *TK* gene containing 8-oxoG was sequenced. I-SceI-induced double strand breaks (DSB) enhanced the gene targeting efficiency by inducing homologous recombination (HR) and resulted in insertion of 8-oxoG into the genome.

revertants were calculated according to the Poisson distribution [31], and *TK* revertants were independently cultured for DNA analysis.

2.6. Mutation analysis at 8-oxoG adduct lesions

High-purity TSCER122 genomic DNAs were isolated from the *TK* revertant clones on 96-microwell plates using DNeasy 96 Blood & Tissue Kits (QIAGEN), and the mutation spectrum of 8-oxoG introduced by pvINT^{8OxG} integration was analyzed (Fig. 3). Subsequently, the *TK* gene fragments containing the 8-oxoG-integration site were amplified by PCR using KOD FX polymerase with the forward and reverse primers: (Pri#291, intron 4), 5′-GCT CTT ACG GAA AAG GAA ACA GG-3′; (Pri#292, intron 5), 5′-CTG ATT CAC AAG CACTGA AG-3′, respectively. PCR amplification was performed with denaturation at 96 °C for 5 min followed by 25 cycles of 96 °C for 30s, 57 °C for 30s, and 68 °C for 1 min. Regions around the *Bss*SI and *MseI*^{R} sites were sequenced using an ABI 3730xl DNA analyzer and clones harboring the *MseI*^{R} sequence were counted to determine the frequency of 8-oxoG integration and numbers of mutations at the *Bss*SI site. Subsequently, the integration frequency of 8-oxoG adducts in the pvINT^{8OxG} targeting vector was calculated by dividing the number of *MseI*^{R} clones by the total number of revertant clones analyzed. Point mutation frequencies opposite the 8-oxoG site were also calculated by dividing the number of single-base substitutions, deletions, and insertions by the number of *MseI*^{R}-bearing clones (Table 1).

2.7. Non-targeting vectors for competitive assays of 8-oxoG repair

Double-stranded (ds) 100-bp DNAs [5′-GGT ACC GGG CCC CCC CTC GAG GTC GAC GGT ATC GAT AAG CTT AGC CTC XTGGGA CTG CAG CCC GGG GGA TCC ACT AGT TCT AGA GCG GCC GCC ACC GCG G (X=G or 8-oxoG)] with nonspecific sequences containing unmodified G or 8-oxoG in *Bss*SI recognition sequences, from Japan Bioservice Corp. (Saitama, Japan). Subsequently, noncompetitive (pvINT^{8OxG} vector and the unmodified 100-bps^G dsDNA) and competitive (pvINT^{8OxG} vector and the 8-oxoG-modified 100-bps^{8OxG} dsDNA) combinations of vectors and dsDNAs were co-transfected in the presence of the I-SceI expression vector (50 μg) into 5 × 10^6 TSCER122 cells using Nucleofector I according to the manufacturer's instructions[27]. The molar ratio between targeting vector and non-targeting vector in both noncompetitive (pvINT^{8OxG}:dsDNA 100-bps^G) and competitive experiments (pvINT^{8OxG}:dsDNA 100-bps^{8OxG}) was approximately 1:60. After transfection, cells were cultured for 3 days and were then seeded into 96-microwell plates in the presence of HAT to isolate 8-oxoG-integrated revertant clones. Drug-resistant colonies were then counted 2 weeks later and were independently cultured for sequencing analysis.

2.8. The TATAM system for 8-oxoG adducts in TS of the TK gene

Initially, 8-oxoG was introduced into NTS of the *TK* gene according to the TATAM system. To compare the mutation properties of 8-oxoG between NTS and TS of the *TK* gene, we also prepared a pvIT^{8OxG} targeting vector for the TS of the *TK* gene. An oligonucleotide primer (R2) containing 8-oxoG was then synthesized (Supplementary Fig. S1) and the pvIT^{8OxG}-targeting vector for TS was prepared as described above.

3. Results

3.1. Preparation of the 8-oxoG-modified targeting vector

We prepared pvINT^{8OxG} and pvINT^G targeting vectors using synthetic 8-oxoG-modified and unmodified primers, respectively, as starting materials (Fig. 2). DNA sequencing confirmed the absence of errors in the entire 6.1-kbp targeting vectors sequence. A stalled peak was also detected at the 8-oxoG-neighboring base site of the pvINT^{8OxG} vector, but not at the same site in the pvINT^G vector (Supplementary Fig. S2), indicating that 8-oxoG adduct was present at the expected site in pvINT^{8OxG} vector, and pvINT^G vector can be used as control.

3.2. Frequency of TK revertant TSCER122 cells in the TATAM system

TSCER122 cells (*TK*−/−) are compound heterozygous for *TK* because of a 356-bp deletion of exon 5 on one *TK* allele, and a point

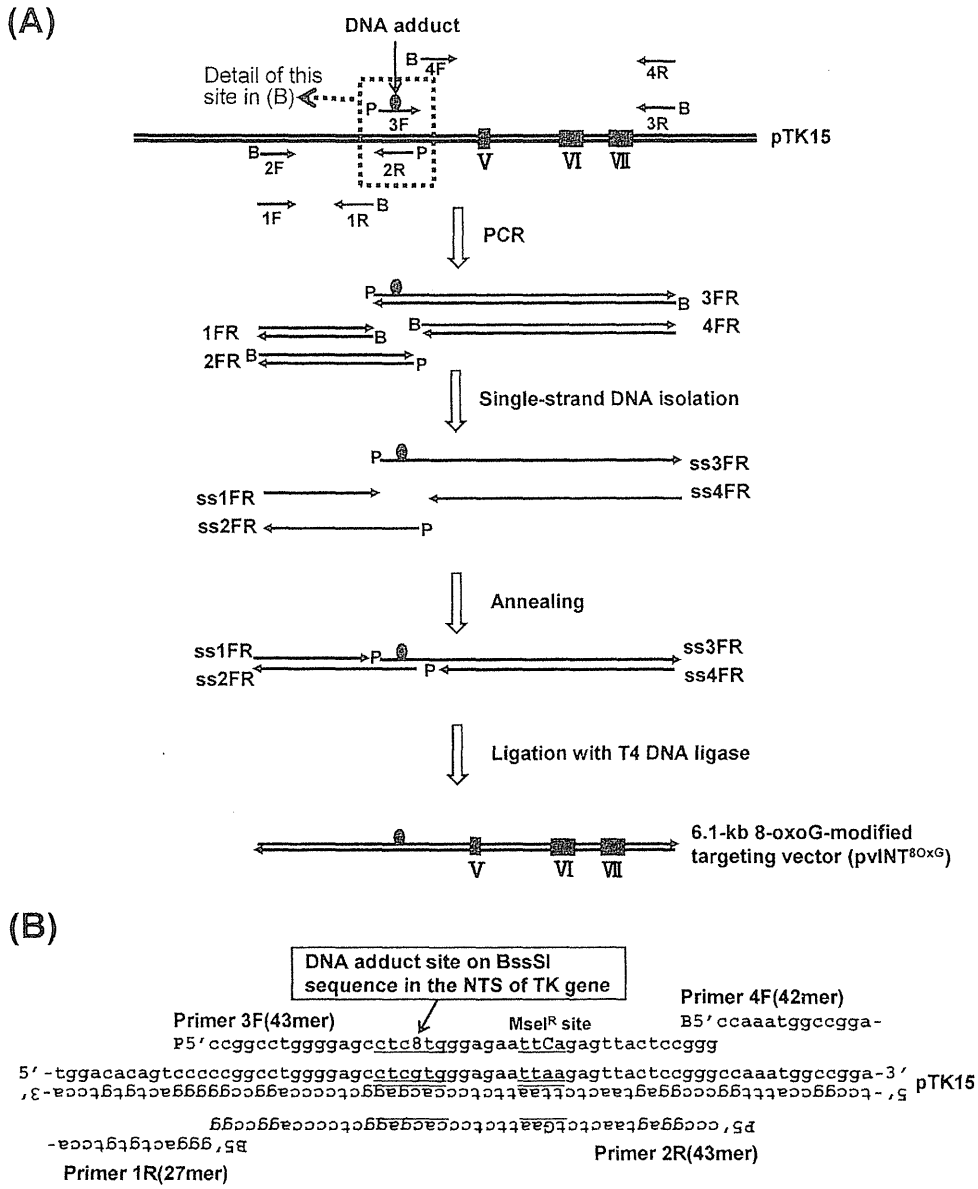

Fig. 2. PCR-based construction of a targeting vector containing a single 8-oxoG. (A) Diagram of pvINT^{8OxG} vector preparation; The P and B at the 5′-terminus of the oligodeoxynucleotides indicate phosphorylation and biotinylation, respectively. (B) Details of the site of 8-oxoG modification; the adduct is indicated by "8" in Primer 3F. We inserted 8-oxoG in place of the central guanine at the *BssSI* site in *TK*-NTS (5′-CTCGTG in Primer 3F) to generate the pvINT^{8OxG} vector. The *MseI*^{R} site was also placed near the site in the 3F and 2R primers.

mutation in exon 4 on the other *TK* allele. An I-*Sce*I site exists on the original exon 5 region (Fig. 3A), which allows generation of wild-type *TK* by correct targeting using pvINT^{8OxG} or pvINT^{G} vectors. Subsequently, *TK* revertant clones (*TK*+/−) can be selected using HAT (Fig. 3B). Gene targeting only with pvINT^{G} vector yielded a very low frequency of *TK* revertants (10^{-7}). In contrast, co-transfection with pvINT^{8OxG} or pvINT^{G} vectors and the I-*Sce*I expression vector pCBASce increased the frequency of *TK* revertants to approximately 10^{-2} (Fig. 4A), indicating that HR-mediated repair of DSB at the I-*Sce*I site enhances targeting efficiency. Interestingly, *TK* revertant frequencies did not differ between cells transfected with pvINT^{8OxG} and pvINT^{G} vectors, indicating that the 8-oxoG adduct in the targeting vector was efficiently delivered to the genome (Fig. 4A). Moreover, in cells transfected with only pCBASce, revertant frequencies were significantly increased from 10^{-4} to 10^{-3} [18–20] (Fig. 4A), indicating that approximately 10% of *TK* revertants in the TATAM system are generated by inter-allelic HR, but not by gene targeting. These revertants were distinguished using the molecular analyses reported below.

TK revertant frequencies were constant until 72 h (Fig. 4B), suggesting that the targeting vector is integrated immediately into the TSCER122 genome. Moreover, *TK* revertant clones increased linearly with quantities of pvINT^{G} targeting vector in the TATAM system (Fig. 4C), indicating that under the present conditions the TATAM system is quantitative and reproducible.

3.3. Determination of mutation frequencies and spectra at integrated 8-oxoG lesions

Table 1 shows mutation frequencies and spectra associated with integration of single 8-oxoG adducts by each targeting vector. The frequencies of pvINT^{G}- (770/888 or 88%) and pvINT^{8OxG}-targeted

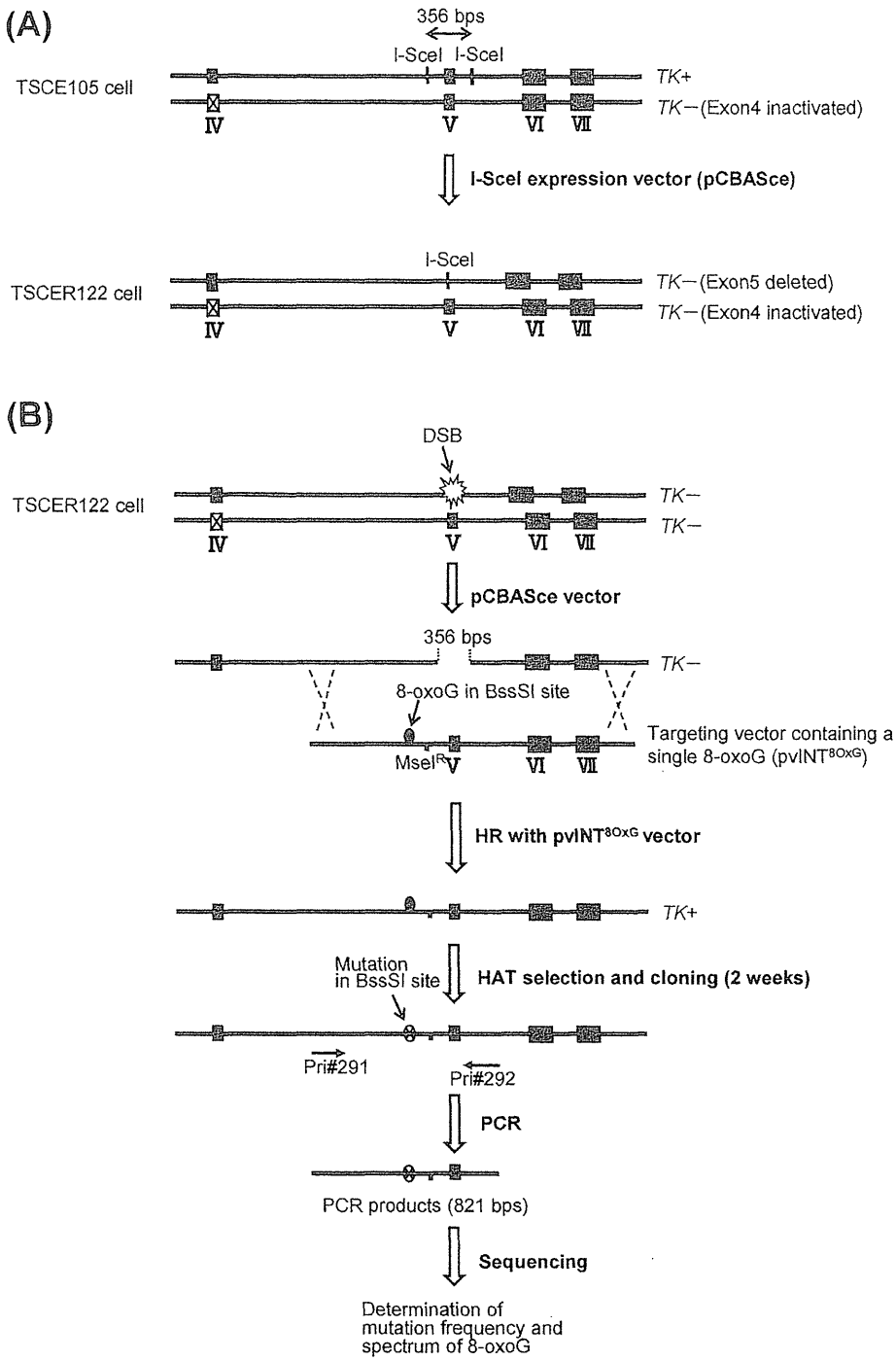

Fig. 3. (A) Development of TSCER122 cells used in the TATAM system. TSCE105 (*TK*+/−) is heterozygous for a point mutation in exon 4 of the *TK* gene and has two I-*Sce*I recognition sites surrounding exon 5 of the *TK*+ allele. Following transfection of the I-*Sce*I expressing vector, DSB occurring at the two I-*Sce*I sites were correctly fused by error-free end-joining and produced a new I-*Sce*I site with a 356-bp deletion containing the entire exon 5, resulting in the *TK*-deficient mutant TSCER122. (B) Principle of the use of HR in the TATAM system. The 8-oxoG-modified targeting vector pvINT^{8OxG} (or pvINT^{G} as a control) and the I-SceI expression plasmid pCBASce were co-transfected into TSCER122 cells. The DSB occurring at the I-*Sce*I site enabled high gene targeting efficiency for the TATAM system by inducing DSB-repair enhanced site-specific HR. The targeting vectors contained *Mse*I^{R} sites, which do not exist in the native *TK* gene and thereby distinguish between targeted and nontargeted revertants. Genomic DNAs were extracted from the clones, and the part of the *TK* gene containing the 8-oxoG-integrated site was amplified by PCR using the primers Pri#291 and #292, as described in Section 2. PCR products were then sequenced using an ABI 3730xl DNA analyzer.

revertants (803/944 or 85%) were similar, and other non-target revertants generated by inter-allelic HR (12% for pvINT^{G} and 15% for pvINT^{8OxG}). These target and non-target revertants were distinguished using *Mse*I enzyme cleavage analyses (Fig. 2B).

Among the sequenced sites generated by integration of 8-oxoG, 86% were repaired or bypassed without causing mutations. Among the remaining 14% of mutations, G:C to T:A transversions were predominant (5.9%), followed by single-base deletions

Table 1
Mutation frequency and spectrum associated with a single integrated 8-oxoG.

Targeting vector	Cell	Experiment	No. of *TK* revertants analyzed	No. of G- or 8-oxoG-integrated revertants	No. of targeted mutants (G or 8-oxoG→X)						Total of point mutation	Others[d]	ND[e]
					Point mutation								
					X=G	T	C	A	Del.[b]	Ins.[c]			
pvINT^{G}	TSCER122	1	250	209	206	0	0	0	0	0		3	0
		2	638	561	551	0	0	0	0	1		9	0
		Total	888	770 (100%)	757 (98%)	0	0	0	0	1 (0.1%)	1 (0.1%)	12	0
pvINT^{8OxG}	TSCER122	1	259	207	176	13	2	1	4	2		5	4
		2	685	596	516	34	8	5	13	4		13	3
		Total	944	803 (100%)	692 (86%)	47 (5.9%)	10 (1.2%)	6 (0.7%)	17 (2.1%)	6 (0.7%)	86 (10.7%)[a]	18	7
pvINT^{8OxG}	TSCER122MYH	1	245	199	171	5	3	1	7	2		7	3
		2	374	308	276	8	5	4	8	1		5	1
		Total	619	507 (100%)	447 (88%)	13 (2.6%)	8 (1.6%)	5 (1%)	15 (2.9%)	3 (0.6%)	44 (8.7%)[a]	12	4

[a] Significantly different from the control value; $P < 0.05$ (Student's *t*-test).
[b] Indicates targeted single-base deletion.
[c] Indicates the sum of targeted C, T, and G insertions.
[d] Non-targeted mutations. See sequence changes shown in Table 2.
[e] Not detectable.

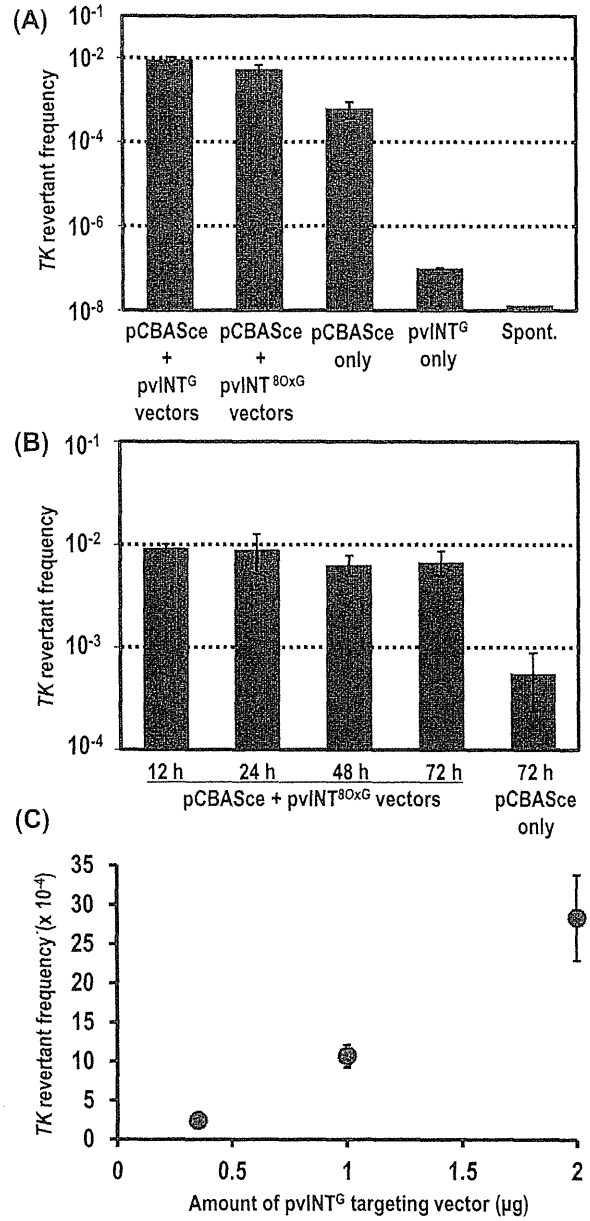

Fig. 4. *TK* revertant frequencies induced by pCBASce and targeting vectors. (A) I-*Sce*I expression vector (pCBASce) and/or pvINT^{8OxG} vector (or pvINT^{G} as a control) were transfected into TSCER122 cells. Three days later, cells were seeded into 96-microwell plates in the presence of HAT to select for *TK*-revertant clones. Two weeks later, microwells containing drug-resistant colonies were counted, and *TK*-revertant frequencies were calculated. (B) No effect of expression period on the frequency of *TK*-revertants; after transfection, cells were cultured for 12, 24, 48, or 72 h, and were then seeded into 96-microwell plates. (C) Dose-dependent relationship between *TK*-revertant frequency and the amount of pvINT^{G} targeting vector; pCBASce (50 μg) and pvINT^{G} (0.4, 1, or 2 μg) vectors were co-transfected into TSCER122 cells and *TK*-revertant frequency increased linearly with increasing quantities of pvINT^{G} targeting vector.

Table 2
Properties of miscellaneous base changes and large deletions at BssSI site.

Other base-changes[a]	pvINT^{G}	pvINT^{8OxG}	
	TSCER122	TSCER122	TSCER122MYH
5′-ctc8tg (original)			
5′-cttgtg	6	1	2
5′-ctcgag	1	1	1
5′-cccgtg	2	2	
5′-ctcgta	1	1	
5′-cttcgtg	2		1
5′-ctctttg		1	2
5′-cccttg		1	
5′-ctattg		1	
5′-ctcgΔg		1	
5′-ctggtg		2	
5′-ctcgttg		2	
5′-ctcgtcg		1	
5′-ctctgg		1	
5′-ctcttgg			1
5′-cttctg			2
5′-ctcattg			1
5′-ttcttg			1
5′-ctctatg			1
135-bp deletion		1[b]	
6-bp deletion		1[c]	
33-bp deletion		1[d]	
Total	12	18	12

[a] "8" and "Δ" indicate 8-oxoG and single-base deletion, respectively.
[b] 5′-gctgcgcagttgtggatgtacctgtcgtctgctgggggcgtgcgggtggacacagtcccccggcctggggagcctcgtgggagaattaagagttactccgggccaaatggccggagttgtcagatccattacc.
[c] 5′-cctcgt.
[d] 5′-gagcctcgtgggagaattaagagttactccggg.

(2.1%) and G:C to C:G transversions (1.2%). In contrast, control vector integrated lesions did not produce any point mutations. Table 2 shows the miscellaneous base changes observed at low frequency. Base substitutions, single-base deletions and insertions were observed around the 8-oxoG sites. Some of these mutations were also observed in the control experiment (pvINT^{G}). However, three deletional mutations (6, 33, and 135-bp) containing 8-oxoG site observed in cells transfected only with pvINT^{8OxG}.

3.4. Stability of 8-oxoG in pvINT^{8OxG} before targeting integration

DNA repair enzymes such as 8-oxoguanine glycosylase (OGG1) may remove 8-oxoG adducts after transfection of plasmid vectors before integration into the genome [28,32,33]. Thus, assays were performed with competitive 100-bps^{8OxG} and noncompetitive 100-bps^{G} vectors that cannot act as targeting vectors. In these experiments, if the 8-oxoG adduct is efficiently excised from the vectors, the revertant frequency with the competitive vector should be higher than with the non-competitive vector. However, the frequencies of base changes in the *Bss*SI cleavage site, which was not present in the revertants (Fig. 3B), were 18.7 ± 2.0% (26/139) for the noncompetitive vector and 14.3 ± 2.3% (19/132) for the competitive vector. These frequencies did not differ significantly, indicating that 8-oxoG was not efficiently excised from the targeting vector prior to integration into the genome.

3.5. Decreased mutation frequencies of 8-oxoG in TSCER122MYH cells

MYH-overexpressing TSCER122MYH cells were isolated from 5×10^6 TSCER122 cells transfected with *Xmn*I-linearized pCI-MYHβ3 and cultured in 96-microwell plates in the presence of G418, as described in Section 2. MYH expression was 2.1-times higher in TSCER122MYH cells than in wild-type TSCER122 cells (Supplementary Fig. S3). Among the 619 genomic DNAs extracted from TSCER122MYH clones, 507 (82%) were *Mse*I^{R}-bearing clones, indicating that the integration frequency was similar to that of the control (Table 1). The total point mutation frequency (8.7%) decreased a little, but did not differ significantly from that in wild-type TSCER122 cells (10.7%). However, the fraction of G:C to T:A transversions in TSCER122MYH cells (2.6%) was 2.3 times lower than in wild-type cells (5.9%; Table 1).

3.6. 8-oxoG mutations did not differ between NTS and TS of the TK gene

Initially, the TATAM system was devised for NTS of the *TK* gene. Subsequently, we analyzed consequences of 8-oxoG adducts in both NTS and TS of the *TK* gene (Table 3). Introduction of 8-oxoG into the *TK*-TS side of the *Bss*SI site (Supplementary Fig. S1) caused a total point mutation frequency of 10.6%, which was similar to that in the NTS side (10.7%). Mutation spectra were also similar between NTS and TS of the *TK* gene. Interestingly, no single-base deletions were detected in the TS side, whereas the frequency of single-base deletions at the NTS side was 2.1% (Table 3).

4. Discussion

Because the frequency of HR in mammalian cells is generally low, the gene targeting efficiency through HR is $<10^{-6}$ [34,35]. In contrast, gene targeting integration using the present TATAM system (Figs. 1 and 3) was 10^{-3} to 10^{-2} (Fig. 4). This dramatic enhancement of gene targeting efficiency was achieved by site-specific I-*Sce*I, which produces DSB that strongly initiates HR [24,25]. In addition, *TK* revertant frequencies increased linearly with the quantity of targeting vector (Fig. 4C), indicating that gene targeting in the TATAM system is not saturated by the targeting vector under the present conditions, enabling quantitative comparison of the gene targeting efficiencies. Using a new PCR-based method, we prepared high yields (micrograms) of target vectors containing DNA adducts within 5 days. Thus, the TATAM system allows efficient recovery of adduct-integrated clones, and can be used to investigate the genetic consequences of individual adducts at specific sites in the human genome.

Oxidative damage by reactive oxygen species (ROS) occurs frequently in all organisms. Reactions of ROS with DNA produce a large variety of lesions on bases and sugars. Among these, the biological importance of 8-oxoG is widely accepted because of its abundance and mutagenicity [36]. The mutagenicity of 8-oxoG has been well characterized in bacterial and mammalian cells. Specifically, shuttle vectors carrying specific 8-oxoG sites predominantly produce G:C to T:A transversions in *E. coli* and simian kidney cells (COS-7) [15,37]. Kamiya et al. integrated a synthetic c-Ha-ras protooncogene containing 8-hydroxyguanine (8-ohG; hydroxyl form of 8-oxoG) in the second position of codon 12 (GGC) into the murine genome of NIH3T3 cells and demonstrated a preponderance of G:C to T:A transversions among the resulting transformants [38]. In another study, treatments of *Ogg1* deficient *gpt* transgenic mice with the oxidative agent potassium bromate ($KBrO_3$) caused tremendous accumulation of 8-ohG lesions in kidney DNA, which produced a high frequency of mutations in the *gpt* gene [39]. Subsequent mutational spectra analyses revealed that G:C to T:A transversions were the most prevalent, followed by G:C to A:T transitions and small deletions in both wild-type and *Ogg1* deficient *gpt* transgenic mice.

The TATAM system showed that 8-oxoG predominantly caused G:C to T:A transversions followed by single base deletions. These

Table 3
Comparison of mutation specificities of a single 8-oxoG placed in the NTS and TS of inherent *TK* gene.

Targeting vector and location of 8-oxoG[a]	No. of *TK* revertants analyzed	No. of 8-oxoG-integrated revertants	No. of targeted mutants (8-oxoG→X)						Total of point mutation	Others[e]	ND[f]
			X=G	Point mutation			Del.[c]	Ins.[d]			
				T	C	A					
pvINT^{8oxoG} 5′ agcctc8tggga tcgcgagagc 3′	944[b]	803 (100%)	692 (86%)	47 (5.9%)	10 (1.2%)	6 (0.7%)	17 (2.1%)	6 (0.7%)	86 (10.7%)	18	7
pvIT^{8oxoG} 5′ agcctcgtggga tcgcgagagc 3′	436	368 (100%)	315 (85%)	29 (7.9%)	8 (2.2%)	1 (0.3%)	0	1 (0.3%)	39 (10.6%)	6	8

[a] "8" indicates 8-oxoG.
[b] Data are taken from Table 1.
[c] Indicates targeted single-base deletions.
[d] Indicates the sum of targeted C, T, and G insertions.
[e] Non-targeted mutations.
[f] Not detectable.

data are consistent with the above reports. However, only 14% of 8-oxoG lesions led to mutations in the system and the remaining 86% of 8-oxoG lesions were restored to G, probably through base excision repair (BER) or TLS (Table 1). Because we did not use drug selection to isolate mutants, the TATAM system enabled both characterization of mutations and evaluation of the efficiency of DNA repair and TLS. To investigate the effects of BER, we constructed TSCER122MYH cells overexpressing the MYH protein, which removes adenine from 8-oxoG:A but not cytosine from 8-oxoG:C [29,40]. Overexpressed MYH only works for 8-oxoG:A that is generated by error-prone TLS. Accordingly, mutation frequencies of G:C to T:A transversions were significantly suppressed in TSCER122MYH cells (2.6%), whereas other mutations occurred with similar frequency, suggesting that MYH in the TATAM system specifically removes adenine from 8-oxoG:A mismatched pairs. These results indicate that the 8-oxoG sites introduced by the TATAM system are processed as those generated by oxidative DNA damage. Use of additional cell types with overexpressed or deficient repair enzymes in the TATAM system will further elucidate DNA repair and TLS mechanisms.

In the present study, the TATAM system characterized mutations induced by xanthine and 8-bromoguanine adducts, which are formed by reactions of ROS and reactive nitrogen species with guanine bases in inflamed tissues [41–43]. As shown in Supplementary Table S1, the predominant mutations (G:C to A:T transitions for xanthine and single-base deletions for 8-bromoguanine) observed in the TATAM system were consistent with previous *in vitro* studies [5,44–46]. Thus, the TATAM system accurately characterizes mutation spectra of various endogenous DNA adducts in the human genome.

In this study, we investigated mutational properties of 8-oxoG on TS and NTS of the *TK* gene using the TATAM system. It is widely accepted that transcription-coupled repair (TCR) is initiated upon irreversible stalling of RNA polymerase II on TS of bulky pyrimidine dimers [47–49]. However, the mechanisms of transcriptional arrest at site-specific 8-oxoG adducts remain unknown. Although pauses and partial blockage by the lesions has been demonstrated using purified RNA polymerase II *in vitro* [50,51], other studies show efficient bypass of 8-oxoG lesions using cell extracts and luciferase reporter assays [52–54]. Pastoriza-Gallego et al. showed that transcriptional arrest by 8-oxoG can vary with proximal promoter strengths and nucleotide sequences [54]. As shown in Table 3, the mutational properties of 8-oxoG on NTS and TS were almost the same, indicating that no preferential strand repair of 8-oxoG adducts in the *TK* gene, and implying that the TCR pathway is not initiated by such lesions.

Interestingly, single-base deletions were detected on NTS, but not on TS in the *TK* gene, potentially reflecting the sequence context of neighboring 8-oxoG rather than the TCR pathway. In a previous study of mammalian cells, oligonucleotides containing 8-oxoG in shuttle vector systems predominantly produced G:C to T:A transversions, whereas other frequently detected mutations were influenced by neighboring sequences and no single base deletions were observed [55]. Thus, the mechanisms behind 8-oxoG-associated single-base deletions in the present TATAM experiments remain unclear. In *in vitro* DNA synthesis experiments using synthetic templates, single-base deletions were generated depending on the neighboring sequences and the polymerase used (mammalian DNA polymerase α, β, and γ, and *E. coli* Klenow fragment pol I or pol III) [56–58]. In contrast, single-base deletions, particularly of guanine, were infrequently observed in transgenic gene mutation assays after treatment of animals with $KBrO_3$ [59]. The TATAM system detects unique mutations caused by 8-oxoG (Table 2, 3). Because some mutations were also produced by the control targeting vector pvINT^{G}, artifactual effects of gene targeting may cause occasional gene mutations. However, some mutations,

particularly large deletions (6–135 bp), were only specifically generated by the pvINT^{8OxG} vector (Table 3), implying an association with DSB. In the BER pathway, 8-oxoG is excised by DNA glycosylase and creates an abasic site, which is incised by AP endonucleases and generates single strand breaks. Repair of these lesions can lead to DSB through collapsed replication forks during cell cycle progression [60]. Hence introduction of DNA adducts into introns of the *TK* gene using the TATAM system enables rescue from various genetic consequences of DNA adducts, such as large deletions, offering a significant advantage for investigations of mutation spectra, and evading selection biases.

In conclusion, the TATAM system we developed here can be used to introduce any synthetic DNA adduct into specific regions of the human genome, providing a valuable tool for quantitative investigations of the fate of individual adducts in the human genome. Moreover, this method can be used to determine the biological characteristics and phenomena of DNA adducts in human cells overexpressing or deficient in specific enzymes, such as DNA polymerases and DNA repair proteins.

Conflict of interest

The authors declare that there are no conflicts of interest.

Acknowledgements

We acknowledge several helpful discussions with Dr. Takehiko Nohmi and Dr. Katsuyoshi Horibata (National Institute of Health Sciences). This work was supported by the Grant-in-Aid for Scientific Research (B) from the Ministry of Education, Culture, Sports, Science and Technology and for Health Science Foundation (H24-food-general-011) from the Ministry of Health, Welfare and Labor in Japan.

Appendix A. Supplementary data

Supplementary data associated with this article can be found, in the online version, at http://dx.doi.org/10.1016/j.dnarep.2014.01.003.

References

[1] T. Lindahl, Instability and decay of the primary structure of DNA, Nature 362 (1993) 709–715.
[2] T.A. Kunkel, The high cost of living, in: American Association for Cancer Research Special Conference: Endogenous Sources of Mutations, Fort Myers, FL, USA, 11–15 November 1998, Trends in Genetics: TIG 15 (1999) 93–94.
[3] P.H. Chou, S. Kageyama, S. Matsuda, K. Kanemoto, Y. Sasada, M. Oka, K. Shinmura, H. Mori, K. Kawai, H. Kasai, H. Sugimura, T. Matsuda, Detection of lipid peroxidation-induced DNA adducts caused by 4-oxo-2(E)-nonenal and 4-oxo-2(E)-hexenal in human autopsy tissues, Chemical Research in Toxicology 23 (2010) 1442–1448.
[4] R.A. Kanaly, S. Matsui, T. Hanaoka, T. Matsuda, Application of the adductome approach to assess intertissue DNA damage variations in human lung and esophagus, Mutation Research 625 (2007) 83–93.
[5] A. Sassa, T. Ohta, T. Nohmi, M. Honma, M. Yasui, Mutational specificities of brominated DNA adducts catalyzed by human DNA polymerases, Journal of Molecular Biology 406 (2011) 679–686.
[6] R.D. Wood, DNA repair in eukaryotes, Annual Review of Biochemistry 65 (1996) 135–167.
[7] C. Masutani, R. Kusumoto, A. Yamada, N. Dohmae, M. Yokoi, M. Yuasa, M. Araki, S. Iwai, K. Takio, F. Hanaoka, The XPV (xeroderma pigmentosum variant) gene encodes human DNA polymerase eta, Nature 399 (1999) 700–704.
[8] D.R. Spitz, E.I. Azzam, J.J. Li, D. Gius, Metabolic oxidation/reduction reactions and cellular responses to ionizing radiation: a unifying concept in stress response biology, Cancer Metastasis Reviews 23 (2004) 311–322.
[9] J.C. Delaney, J.M. Essigmann, Biological properties of single chemical-DNA adducts: a twenty year perspective, Chemical Research in Toxicology 21 (2008) 232–252.
[10] J.M. Essigmann, C.L. Green, R.G. Croy, K.W. Fowler, G.H. Buchi, G.N. Wogan, Interactions of aflatoxin B1 and alkylating agents with DNA: structural and functional studies, Cold Spring Harbor Symposia on Quantitative Biology 47 (Pt 1) (1983) 327–337.
[11] N. Shrivastav, D. Li, J.M. Essigmann, Chemical biology of mutagenesis and DNA repair: cellular responses to DNA alkylation, Carcinogenesis 31 (2010) 59–70.
[12] A.K. Basu, J.M. Essigmann, Site-specifically modified oligodeoxynucleotides as probes for the structural and biological effects of DNA-damaging agents, Chemical Research in Toxicology 1 (1988) 1–18.
[13] E.L. Loechler, C.L. Green, J.M. Essigmann, In vivo mutagenesis by O^6-methylguanine built into a unique site in a viral genome, Proceedings of the National Academy of Sciences of the United States of America 81 (1984) 6271–6275.
[14] A.K. Basu, E.L. Loechler, S.A. Leadon, J.M. Essigmann, Genetic effects of thymine glycol: site-specific mutagenesis and molecular modeling studies, Proceedings of the National Academy of Sciences of the United States of America 86 (1989) 7677–7681.
[15] M. Moriya, Single-stranded shuttle phagemid for mutagenesis studies in mammalian cells: 8-oxoguanine in DNA induces targeted G.C→T.A. transversions in simian kidney cells, Proceedings of the National Academy of Sciences of the United States of America 90 (1993) 1122–1126.
[16] H. Nishida, M. Kawanishi, T. Takamura-Enya, T. Yagi, Mutagenic specificity of N-acetoxy-3-aminobenzanthrone, a major metabolically activated form of 3-nitrobenzanthrone, in shuttle vector plasmids propagated in human cells, Mutation Research 654 (2008) 82–87.
[17] K.C. Cheng, D.S. Cahill, H. Kasai, S. Nishimura, L.A. Loeb, 8-Hydroxyguanine, an abundant form of oxidative DNA damage, causes G–T and A–C substitutions, Journal of Biological Chemistry 267 (1992) 166–172.
[18] K.S. Ellison, E. Dogliotti, T.D. Connors, A.K. Basu, J.M. Essigmann, Site-specific mutagenesis by O^6-alkylguanines located in the chromosomes of mammalian cells: influence of the mammalian O^6-alkylguanine-DNA alkyltransferase, Proceedings of the National Academy of Sciences of the United States of America 86 (1989) 8620–8624.
[19] K.B. Altshuler, C.S. Hodes, J.M. Essigmann, Intrachromosomal probes for mutagenesis by alkylated DNA bases replicated in mammalian cells: a comparison of the mutagenicities of O^4-methylthymine and O^6-methylguanine in cells with different DNA repair backgrounds, Chemical Research in Toxicology 9 (1996) 980–987.
[20] L. Izhar, O. Ziv, I.S. Cohen, N.E. Geacintov, Z. Livneh, Genomic assay reveals tolerance of DNA damage by both translesion DNA synthesis and homology-dependent repair in mammalian cells, Proceedings of the National Academy of Sciences of the United States of America 110 (2013) E1462–E1469.
[21] M. Honma, M. Izumi, M. Sakuraba, S. Tadokoro, H. Sakamoto, W. Wang, F. Yatagai, M. Hayashi, Deletion, rearrangement, and gene conversion; genetic consequences of chromosomal double-strand breaks in human cells, Environmental and Molecular Mutagenesis 42 (2003) 288–298.
[22] M. Honma, M. Sakuraba, T. Koizumi, Y. Takashima, H. Sakamoto, M. Hayashi, Non-homologous end-joining for repairing I-SceI-induced DNA double strand breaks in human cells, DNA Repair (Amsterdam) 6 (2007) 781–788.
[23] Y. Takashima, M. Sakuraba, T. Koizumi, H. Sakamoto, M. Hayashi, M. Honma, Dependence of DNA double strand break repair pathways on cell cycle phase in human lymphoblastoid cells, Environmental and Molecular Mutagenesis 50 (2009) 815–822.
[24] P. Rouet, F. Smih, M. Jasin, Expression of a site-specific endonuclease stimulates homologous recombination in mammalian cells, Proceedings of the National Academy of Sciences of the United States of America 91 (1994) 6064–6068.
[25] M. Porteus, Homologous recombination-based gene therapy for the primary immunodeficiencies, Annals of the New York Academy of Sciences 1246 (2011) 131–140.
[26] A.J. Grosovsky, B.N. Walter, C.R. Giver, DNA-sequence specificity of mutations at the human thymidine kinase locus, Mutation Research 289 (1993) 231–243.
[27] K. Maasho, A. Marusina, N.M. Reynolds, J.E. Coligan, F. Borrego, Efficient gene transfer into the human natural killer cell line, NKL, using the Amaxa nucleofection system, Journal of Immunological Methods 284 (2004) 133–140.
[28] T. Ohtsubo, K. Nishioka, Y. Imaiso, S. Iwai, H. Shimokawa, H. Oda, T. Fujiwara, Y. Nakabeppu, Identification of human MutY homolog (hMYH) as a repair enzyme for 2-hydroxyadenine in DNA and detection of multiple forms of hMYH located in nuclei and mitochondria, Nucleic Acids Research 28 (2000) 1355–1364.
[29] M. Takao, Q.M. Zhang, S. Yonei, A. Yasui, Differential subcellular localization of human MutY homolog (hMYH) and the functional activity of adenine:8-oxoguanine DNA glycosylase, Nucleic Acids Research 27 (1999) 3638–3644.
[30] T. Arakawa, T. Ohta, Y. Abiko, M. Okayama, I. Mizoguchi, T. Takuma, A polymerase chain reaction-based method for constructing a linear vector with site-specific DNA methylation, Analytical Biochemistry 416 (2011) 211–217.
[31] E.E. Furth, W.G. Thilly, B.W. Penman, H.L. Liber, W.M. Rand, Quantitative assay for mutation in diploid human lymphoblasts using microtiter plates, Analytical Biochemistry 110 (1981) 1–8.
[32] K. Nishioka, T. Ohtsubo, H. Oda, T. Fujiwara, D. Kang, K. Sugimachi, Y. Nakabeppu, Expression and differential intracellular localization of two major forms of human 8-oxoguanine DNA glycosylase encoded by alternatively spliced OGG1 mRNAs, Molecular Biology of the Cell 10 (1999) 1637–1652.
[33] H. Ide, M. Kotera, Human DNA glycosylases involved in the repair of oxidatively damaged DNA, Biological and Pharmaceutical Bulletin 27 (2004) 480–485.
[34] K.M. Vasquez, K. Marburger, Z. Intody, J.H. Wilson, Manipulating the mammalian genome by homologous recombination, Proceedings of the National Academy of Sciences of the United States of America 98 (2001) 8403–8410.
[35] S. So, Y. Nomura, N. Adachi, Y. Kobayashi, T. Hori, Y. Kurihara, H. Koyama, Enhanced gene targeting efficiency by siRNA that silences the expression of the Bloom syndrome gene in human cells, Genes to Cells 11 (2006) 363–371.